THE JOURNAL OF COMPARATIVE NEUROLOGY 503:466–485 (2007)

Changes in Vesicular Transporters for γ-Aminobutyric Acid and Glutamate Reveal Vulnerability and Reorganization of Hippocampal Neurons Following Pilocarpine-Induced Seizures

JEAN-LUC BOULLAND,[1] LOTFI FERHAT,[2] TOM TALLAK SOLBU,[1] NADINE FERRAND,[2] FARRUKH ABBAS CHAUDHRY,[1,3] JON STORM-MATHISEN,[3] AND MONIQUE ESCLAPEZ[2,4,5]*

[1]The Biotechnology Centre of Oslo, University of Oslo, Oslo, N-0349 Norway
[2]Institut National de la Santé et de la Recherche Médicale U29, INMED, Marseille, F-13009 France
[3]Department of Anatomy, Institute of Basic Medical Sciences and Centre for Molecular Biology and Neuroscience, University of Oslo, Oslo, N-0317 Norway
[4]Institut National de la Santé et de la Recherche Médicale U751, Laboratoire de Neurophysiologie et Neuropsychologie (LNN), Marseille, F-13005 France
[5]Aix-Marseille Université, Faculté de Médecine Timone, Marseille, F-13005 France

ABSTRACT

The reorganizations of the overall intrinsic glutamatergic and γ-aminobutyric acid (GABA)-ergic hippocampal networks as well as the time course of these reorganizations during development of pilocarpine-induced temporal lobe epilepsy were studied with in situ hybridization and immunohistochemistry experiments for the vesicular glutamate transporter 1 (VGLUT1) and the vesicular GABA transporter (VGAT). These transporters are particularly interesting as specific markers for glutamatergic and GABAergic neurons, respectively, whose expression levels could reflect the demand for synaptic transmission and their average activity. We report that 1) concomitantly with the loss of some subpopulations of VGAT-containing neurons, there was an up-regulation of VGAT synthesis in all remaining GABA neurons as early as 1 week after pilocarpine injection. This enhanced synthesis is characterized by marked increases in the relative amount of VGAT mRNAs in interneurons associated with increased intensity of axon terminal labeling for VGAT in all hippocampal layers. 2) There was a striking loss of mossy cells during the latent period, demonstrated by a long-term decrease of VGLUT1 mRNA-containing hilar neurons and associated loss of VGLUT1-containing terminals in the dentate gyrus inner molecular layer. 3) There were aberrant VGLUT1-containing terminals at the chronic stage resulting from axonal sprouting of granule and pyramidal cells. This is illustrated by a recovery of VGLUT1 immunoreactivity

Grant sponsor: Institut National de la Santé et de la Recherche Médicale; Grant sponsor: Norwegian Research Council (to J.-L.B., T.T.S., F.A.C., J.S.-M.); Grant sponsor: European Union; Grant number: QLG3-CT-2001-02004, DECG (to J.S.-M.).

Lotfi Ferhat's current address is Centre National de la Recherche Scientifique, UMR 6184, Neurobiologie des Interactions Cellulaires et Neurophysiopathologie (NICN), IFR Jean Roche, Marseille, F-13020 France.

*Correspondence to: Dr. Monique Esclapez, INSERM U751, Faculté de Médecine Timone, 27 boulevard Jean Moulin, 13385 Marseille Cedex 05, France. E-mail: monique.esclapez@medecine.univ-mrs.fr

Received 26 September 2006; Revised 21 February 2007; Accepted 10 March 2007

DOI 10.1002/cne.21384

Published online in Wiley InterScience (www.interscience.wiley.com).

in the inner molecular layer and an increased VGLUT1 immunolabeling in the CA1–CA3 dendritic layers. These data indicate that an increased activity of remaining GABAergic interneurons occurs during the latent period, in parallel with the loss of vulnerable glutamatergic and GABAergic neurons preceding the reorganization of glutamatergic networks. J. Comp. Neurol. 503:466–485, 2007.

Indexing terms: temporal lobe epilepsy; VGLUT1; VGAT; GAD; rat

Several modifications of the glutamatergic and γ-aminobutyric acid (GABA)-ergic hippocampal networks have been described in the pilocarpine model of temporal lobe epilepsy at the chronic stage, when the animals have developed spontaneous recurrent limbic seizures. These modifications include an axonal sprouting and aberrant neosynaptogenesis of the granule cells and CA1 pyramidal neurons (Okazaki et al., 1995; Esclapez et al., 1999; Lehmann et al., 2001; Okazaki and Nadler, 2001; Buckmaster et al., 2002), a loss of specific subpopulations of GABAergic neurons in the hilus of the dentate gyrus (Obenaus et al., 1993; Houser and Esclapez, 1996; Kobayashi and Buckmaster, 2003) and in the stratum oriens of CA1 (Houser and Esclapez, 1996; Dinocourt et al., 2003), and increased activity of remaining GABAergic neurons (Esclapez et al., 1997, 1999; Cossart et al., 2001). Some of these reorganizations start during the latent period (after the initial period of status epilepticus following pilocarpine injection), when the animals display a normal behavior (Obenaus et al., 1993; Dinocourt et al., 2003; Ferhat et al., 2003; Kobayashi and Buckmaster, 2003). However, little is known about the time course of these different structural and physiological modifications during development of this epilepsy. Such information is crucial to determine the critical factors that could lead to the emergence of the first spontaneous seizures. The goal of this study was to assess the structural reorganizations and modifications of presynaptic transmitter packaging capacity of the intrinsic glutamatergic and GABAergic hippocampal networks as well as the time course of these alterations at the different stages of development of pilocarpine-induced epilepsy (latent and chronic stage) by using in situ hybridization and immunohistochemical experiments for the vesicular glutamate transporter 1 (VGLUT1) and the vesicular GABA transporter (VGAT).

Such markers were selected because 1) in the cerebral cortex, including the hippocampal formation, VGLUT1 and VGAT are specific markers for the glutamatergic and GABA networks, respectively (Chaudhry et al., 1998; Fremeau et al., 2001), and 2) their expression levels may reflect the demand for synaptic transmission and likely the average presynaptic activity of these neurons (Fremeau et al., 2004; Wojcik et al., 2004, 2006). In the hippocampal formation, VGLUT1 mRNA and protein are located in the cell body and axon terminals, respectively, of all intrinsic glutamatergic principal cells, including the CA1–CA3 pyramidal cells of Ammon's horn and the granular cells of the dentate gyrus (Bellocchio et al., 1998, 2000; Fremeau et al., 2001; Kaneko et al., 2002). Similarly, VGAT mRNA and protein are restricted to cell body and axon terminals of GABAergic interneurons (McIntire et al., 1997; Chaudhry et al., 1998; Sperk et al., 2003). These vesicular transporters are required for the translocation of the neurotransmitters into synaptic vesicles at axon terminals. After an action potential, synaptic vesicles release their transmitter content into the synaptic cleft. The amount of neurotransmitter released by an action potential at a given synapse is subject to multiple regulatory mechanisms. One of them is the expression level of vesicular transporters that have been shown to regulate the amount of neurotransmitter content into synaptic vesicles (Song et al., 1997; Pothos et al., 2000; Travis et al., 2000; Fremeau et al., 2004; Wojcik et al., 2004, 2006). Therefore, the expression levels of vesicular transporters can influence directly the synaptic performance and reflect an average level of presynaptic activity.

Our data demonstrate that the death of the vulnerable subpopulation of glutamatergic neurons, the hilar mossy cells, occurred in parallel with the death of the vulnerable subpopulations of GABAergic neurons in the stratum oriens of CA1 and in the hilus of the dentate gyrus at the beginning of the latent period, after the status epilepticus induced by pilocarpine injection. In contrast, the reorganizations of the glutamatergic and GABAergic neuronal networks as well as their time course were different. The reorganization of the surviving GABAergic neurons was characterized mainly by an up-regulation of presynaptic molecules involved in GABAergic neurotransmission that likely reflected an increased presynaptic activity, occurred as early as at the beginning of the latent period, and persisted during the chronic stage. The reorganization of the glutamatergic principal neurons corresponds mainly to an axonal sprouting and aberrant synaptogenesis that occurred at the chronic stage.

MATERIALS AND METHODS

Animals

All animal use protocols were approved by the European Communities Council (86/609/EEC). Adult male Wistar rats weighing 200–290 g (Charles River France) were injected intraperitonealy (i.p.) with pilocarpine hydrochloride (340 mg/kg; Sigma, St. Louis, MO), a muscarinic cholinergic agonist. The injection protocols were similar to those previously described (Turski et al., 1983; Cavalheiro et al., 1987; Obenaus et al., 1993). A low dose of the cholinergic antagonist methyl scopolamine nitrate (1 mg/kg, i.p.) was administrated 30 minutes before pilocarpine injection in order to reduce the peripheral effects of the cholinergic agonist (Baez et al., 1976; Turski et al., 1983). Only animals that displayed robust behavioral seizures for 3 hours were selected in this study. This period of severe sustained seizures was stopped by a single injection of diazepam (8 mg/kg, i.p.; Sigma) to reduce mortality of the animals. The rats were then observed periodically in the vivarium for general behavior and occurrence of spontaneous seizures for a period of 16 weeks. Pilocarpine-

treated animals were studied at several postinjection intervals: during the latent period, when animals displayed an apparently normal behavior (1 and 2 weeks, n = 6 at each interval), and during the chronic stage, when the animals have developed spontaneous recurrent limbic seizures (8, 12, and 16 weeks; n = 3 at each interval). We previously demonstrated in this model of pilocarpine-treated rats, by using in vivo electroencephalographic recordings, that the first spontaneous seizures occur during the third week after status epilepticus (El-Hassar et al., 2007). Eight age-matched rats from the same litters were used as controls.

Tissue preparation

The rats were deeply anesthetized with sodium pentobarbital injection (60 mg/kg, i.p.) and perfused intracardially with a fixative solution containing 4% paraformaldehyde in 0.12 M sodium phosphate buffer, pH 7.4 (PB). The rats received 300 ml of this fixative per 100 g body weight. After perfusion, the brains were removed from the skull, postfixed in the same fixative for 1 hour at room temperature (RT), and rinsed in 0.12 M PB for 1.5 hours. Blocks of the forebrain containing the entire hippocampal formation were immersed in a cryoprotective solution of 20% sucrose in PB overnight at 4°C, quickly frozen on dry ice, and sectioned coronally at 40 μm with a cryostat. The sections were rinsed in 0.01 M phosphate-buffered saline (PBS), pH 7.4, collected sequentially in tubes containing an ethylene glycol-based cryoprotective solution (Watson et al., 1986; Lu and Haber, 1992), and stored at –20°C until histological processing.

Every tenth section was stained with cresyl violet to determine the general histological characteristics of the tissue within the rostral-caudal extent of the hippocampal formation. From each rat, adjacent sections were processed for nonradioactive in situ hybridization with VGAT and VGLUT1 cRNA probes and for immunohistochemistry with antibodies that are specific for each vesicular transporter. Sections from control and pilocarpine-treated rats were always processed in parallel.

In situ hybridization

Probe synthesis. The VGAT and VGLUT1 probes used in this study were digoxigenin-labeled riboprobes obtained by in vitro transcription of the following cDNAs. The VGAT cDNA was obtained by RT-PCR. It corresponds to the 52–237 bp fragment of the rat sequence. This cDNA (297 bp) was inserted into the pCR TOPO II vector (Invitrogen, Burlingame, CA) for in vitro transcription. The VGLUT1 cDNA was cloned by RT-PCR. It corresponds to the 1,593–1,915-bp fragment of the rat sequence. This cDNA (322 bp) was inserted into the pCDNA3 vector (Invitrogen) for in vitro transcription.

The transcription was carried out with the nonradioactive RNA labeling kit (Roche Diagnostics, Meylan, France). The recombinant plasmid containing the VGAT cDNA insert was linearized with the restriction enzyme Hind III and transcribed with T7 RNA polymerase to obtain the sense probe or linearized with EcoRV and transcribed with Sp6 to obtained the antisense probe. The plasmid containing the VGLUT1 cDNA insert was linearized with Hind III and transcribed with T7 RNA polymerase to obtained the antisense probe or linearized with EcoRV and transcribed with Sp6 to obtain the sense probe.

The labeling efficiency of the digoxigenin-labeled probes for VGAT or VGLUT1 mRNA was determined each time by direct immunological detection on dot blots with a nucleic acid detection kit (Roche Diagnostics). The intensity of the signal for each probe was compared with a serial dilution of digoxigenin-labeled control RNA of known concentration. Only antisense and sense VGAT and VGLUT1 probes with comparable signal intensity (comparable labeling efficiency), as determined in dot blots, were used for in situ hybridization.

Hybridization and detection. Free-floating sections were processed for VGAT and VGLUT1 in situ hybridization according to a previously described protocol (Esclapez et al., 1993). To enhance penetration of the probes, sections were pretreated with the following solutions: 0.02 N HCl for 10 minutes; 0.01% Triton X-100 in PBS for 3 minutes; and 0.25 μg/ml proteinase K in 50 mM Tris buffer, 5 mM ethylene diamine tetraacetate (EDTA), pH 7.4, for 10 minutes. After these pretreatments, sections were incubated for 1 hour at RT in a prehybridization solution containing 50% formamide, 750 mM NaCl, 25 mM EDTA, 25 mM piperazine-N,N8-bis 2-ethanesulfonic acid (PIPES), 0.02% Ficoll, 0.02% polyvinylpyrrolidone, 0.02% bovine serum albumin (BSA), 0.2% sodium dodecyl sulfate (SDS), 250 μg/ml poly-A, and 250 μg/ml salmon sperm DNA. Sections were then incubated for 16 hours at 50°C in the hybridization solution, consisting of the prehybridization solution with the addition of 0.2 ng/μl digoxigenin labeled RNA probe, 100 mM dithiothreitol (DTT), and 4% dextran sulfate. After hybridization, sections were rinsed in a 4× saline sodium citrate solution (1× SSC: 150 mM NaCl, 60 mM Na citrate, pH 7.0) containing 10 mM sodium thiosulfate and were treated with ribonuclease A (50 μg/ml in 0.5 M NaCl, 10 mM sodium thiosulfate, 1 mM EDTA, 10 mM Tris HCl buffer, pH 8.0) for 30 minutes at 37°C. Low- to high-stringency washes were performed with decreasing concentrations of SSC, ending with an incubation in 0.1× SSC, 10 mM sodium thiosulfate for 30 minutes at 55°C. Sections were then processed for immunodetection of the digoxigenin label by means of a nucleic acid detection kit (Roche Diagnostic). The sections were rinsed twice in 100 mM Tris HCl buffer, 150 mM NaCl, pH 7.5; incubated for 1 hour in the same buffer containing 0.5% blocking reagent and 0.3% Triton X-100; then incubated overnight at 4°C in alkaline phosphatase-conjugated sheep antibodies to digoxigenin diluted 1:1,000 in the same buffer containing 0.3% Triton X-100. On the following day, the sections were rinsed thoroughly and incubated in a chromogen solution containing nitroblue tetrazolium (NBT) and 5-bromo-4-chloro-3-indolyl phosphate (BCIP) reagents (for details see Esclapez et al., 1993).

The times in the chromogen solution were determined according to two different protocols. In one series of experiments, sections from control and pilocarpine-treated animals were incubated in the chromogen solution until optimal staining was achieved for VGAT mRNA and VGLUT1 mRNA in each of the four animal groups (control, 1 week, 2 weeks, and chronic pilocarpine-treated rats). Optimal staining was defined as a maximum number of specifically stained neurons (maximum sensitivity) with a low background of general tissue staining. For VGLUT1 probe, the optimal color-reaction times (5.5 hours) were similar for all sections from all animal groups (control and pilocarpine-treated animals). For VGAT

probe, the optimal color-reaction times were similar for all sections belonging to the same animal group (control or pilocarpine-treated animals) but very different between sections from the control and the pilocarpine groups. The optimal color-reaction times for hippocampal regions of control animals were approximately 47 hours. Optimal color-reaction times always were shorter (approximately 26 hours) for sections from all pilocarpine-treated animals, despite the fact that sections from control and pilocarpine animals were processed in parallel and under identical experimental conditions. Levels of labeling, in relation to the color-reaction times, have been discussed previously and reflect differences in the relative amounts of mRNA (Hoëltke and Kessler, 1990; Esclapez et al., 1993; Esclapez and Houser, 1999). Neurons with higher levels of mRNA are labeled after a shorter time in the chromogen solution than neurons with lower levels of mRNA, when all other conditions are the same (Esclapez and Houser, 1999). A second series of experiments was conducted to compare directly the differences in levels of labeling for mRNA-containing neurons between the four animal groups (control, one week, 2 weeks, and chronic pilocarpine-treated animals). Sections from these groups were incubated for identical times in the chromogen solution. Series of sections from control and pilocarpine-treated animals that were processed identically were removed from the chromogen solution at two time intervals for each probe (e.g., 20 hours and 40 hours for VGAT; 2 hours and 5.5 hours for VGLUT1) to compare the labeling intensities among sections from the four animal groups at each interval.

The differences in the levels of labeling were determined subsequently by qualitative analyses of the intensity of the color-reaction product of VGAT mRNA- or VGLUT1 mRNA-containing hippocampal neurons. In all experiments, the color reaction was stopped by rinsing the sections in 10 mM Tris HCl, pH 8.0, with 1 mM EDTA. Sections were then mounted on gelatin-coated slides, dried, and coverslipped in an aqueous mounting medium (Crystal/Mount; Biomeda, Foster City, CA).

Immunohistochemistry

Primary antibodies. The polyclonal antiserum directed against VGAT (anti-VGAT-N2) was generated by immunization of rabbits with a fusion protein produced in *Escherichia coli* from a construct coding for glutathion-S-transferase (GST) and the C-terminal segment (amino acid residues 508–525) of the VGAT transporter (Chaudhry et al., 1998). The polyclonal antiserum directed against VGLUT1 (anti-VGLUT1) was generated by immunization of rabbits with a fusion protein produced in *E. coli* from a construct coding for GST and the C-terminal segment (amino acid residues 493–560) of the VGLUT1 transporter (Bellocchio et al., 1998). The specificities of the ensuing sera were previously tested on immunoblots of the whole rat brain sodium dodecyl sulfate (SDS) extracts separated by SDS-PAGE and were shown to produce a single band at the expected molecular weight of 50 kDa for VGAT (Chaudhry et al., 1998) and 60 kDa for VGLUT1 (Bellocchio et al., 1998; Boulland et al., 2004).

For multiple immunofluorescence labeling experiments, the VGLUT1 polyclonal antiserum used (AB 5907; Chemicon International, Temecula, CA) was generated by immunization of guinea pigs with a synthetic peptide (amino acid residues 541–560 of the VGLUT1 transporter). This antiserum labels a single band of 60 kDa molecular weight on Western blot (manufacturer's technical information; Boulland and Chaudhry, unpublished data). The pattern of immunohistochemical labeling obtained with the guinea pig anti-VGLUT1 in rodent brain tissue was similar to that obtained with the rabbit anti-VGLUT1 (Persson et al., 2006; Bogen et al., 2006).

A monoclonal antibody directed against the glutamate decarboxylase 65-kDa isoform (MAB 351R; Chemicon International) was used to labeled axon terminals of GABAergic neurons. This antibody was produced by a GAD-6 hybridoma line obtained after immunization of a mouse with rat brain GAD (Chang and Gottlieb, 1988). It specifically recognizes a single band of 65 kDa on Western blots (Chang and Gottlieb, 1988; Esclapez et al., 1994).

Single immunohistochemical labeling for VGLUT1 and VGAT. All free-floating sections were processed for immunohistochemistry as previously described (Boulland et al., 2002). Sections were first rinsed for 3×5 minutes in PB, pretreated for 30 minutes in 1 M ethanolamine-HCl (pH 7.4) in PB followed by 0.1% H_2O_2 prepared in PBS, and rinsed for 20 minutes in Tris-buffered saline (TBS: 0.1 M Tris HCl, 0.3 M NaCl, pH 7.4). Sections were preincubated for 1 hour at RT in TBS containing 0.1% Triton X-100 and 10% newborn calf serum (NCS) and incubated overnight at RT in primary polyclonal antiserum (1:1,000 for anti-VGAT-N2 or 1:3,000 for anti-VGLUT1) diluted in TBS containing 0.1% (w/v) Triton X-100, 1% (v/v) NCS, and 0.1% (w/v) NaN_3. After these steps, sections were rinsed for 20 minutes in the same buffer without NaN_3; incubated for 1 hour at RT in biotinylated donkey anti-rabbit immunoglobulin G (IgG; RPN 1004; Amersham, GE Healthcare, Oslo, Norway) diluted 1:100 in TBS containing 0.1% (w/v) Triton X-100, 1% (v/v) NCS; rinsed in the same buffer for 20 minutes; and incubated for 1 hour at RT with an streptavidin-biotinylated-horseradish peroxidase complex (Amersham; 1:100) prepared in TBS containing 0.1% Triton X-100 (w/v), 1% (v/v) NCS. After 20-minute rinses in 0.01 M PBS, pH 7.4, sections from control and pilocarpine-treated rats were processed for the same time (7 minutes) in 0.06% 3-3′-diaminobenzidine-HCl and 0.01% H_2O_2 diluted in PB. The sections were rinsed for 20 minutes in PBS, mounted between two coverslipped in Glycerin Gelantin (Kaiser, chroma-gesellschaft; Chemi-Teknik, Oslo, Norway).

The specificity of the immunohistochemical labeling was tested for each primary antiserum or antibody 1) by incubating some sections from control and pilocarpine-treated animals in a solution containing rabbit, mouse, or guinea pig normal IgG (Vector, Burlingame, CA), instead of the primary antiserum or antibody, and 2) by incubating some sections in a solution omitting the primary antiserum or antibody. No specific staining was detected under these conditions.

Multiple immunofluorescence labeling for VGLUT1, VGAT, and GAD65. Free-floating sections for control and pilocarpine-treated animals were processed for immunofluorescence as previously described (Boulland et al., 2004). Sections were pretreated for 10 minutes in 1 M ethanolamine-HCl (pH 7.4) in PB; rinsed for 20 minutes in the same buffer; and incubated for 1 hour at RT in 10% (v/v) normal goat serum (NGS), 3% (w/v) BSA, 0.5% (w/v) Triton X-100, 0.05% (w/v) NaN_3 diluted in TBS. Sections were then incubated overnight at RT in a mixture of VGAT antiserum (1:2,000), VGLUT1 antiserum (1:5,000),

and GAD65 antibody (1:1,000) diluted in TBS containing 3% (v/v) NGS, 1% (w/v) BSA, 0.5% (w/v) Triton X-100, 0.05% (w/v) NaN_3 (diluent solution). Sections were washed for 3 × 5 minutes with the diluent solution and incubated for 1 hour in the a mixture of Alexa 488 goat anti-rabbit IgG (Molecular Probes, Eugene, OR; 1:1,000), Alexa 568 goat anti-guinea pig IgG (Molecular Probes; 1:500), and Alexa 633 goat anti-mouse IgG (Molecular Probes; 1:1,000) diluted in TBS containing 3% (v/v) NGS, 1% (w/v) BSA, 0.5% (w/v) Triton X-100. Sections were rinsed for 3 × 5 minutes in PB and mounted on Fluoromount G (Southern Biotechnology Associates, Birmingham, AL).

Immunohistochemical controls for triple-labeling experiments included incubation of some sections in a mixture of one primary antiserum (or antibody) and normal IgG (rabbit/mouse normal IgG, guinea pig/mouse normal IgG or guinea pig/rabbit normal IgG). In all cases, these sections displayed the same pattern of immunolabeling as sections processed for single labeling.

Data acquisition

Sections from control and pilocarpine-treated animals, processed for single-labeling immunohistochemistry or nonradioactive in situ hybridization, were examined with an Eclipse E800 light microscope (Nikon France S.A.S) and photographed with a Nikon DMX 1200 digital camera under the same conditions of light illumination, with the microscope light source stabilized. Sections processed for multiple immunofluorescence labeling were observed with an Axioplan 2 and a Pascal 5 LSM laser scanning confocal microscope (Zeiss). Image scans were obtained with a ×63 oil-immersion lens. A pinhole, adjusted around 1 area unit, was optimized for each laser wavelength to obtain the same optical slice for each wavelength. Double-stained terminals were determined in three dimensions to ensure that the yellow staining observed was not due to a close overlap between two terminals stained with different dyes.

All photomicrographs were cropped and optimized by making minor adjustments to level and contrast/brightness curves to the entire image in Adobe Photoshop CS2 for Macintosh (Adobe, San Jose, CA). The same adjustments were applied to photographs of sections from control and pilocarpine-treated animals. Figure montages were made in Adobe InDesign CS2.

RESULTS

Changes in VGLUT1 mRNA labeling in the hippocampus of pilocarpine-treated rats

In control animals (n = 8/8), all principal cells of the hippocampal formation were labeled for VGLUT1 mRNA, including the pyramidal cells of the CA1, CA2, and CA3 regions of the hippocampus and the granule cells of the dentate gyrus (Fig. 1A) as previously reported for rodents (Fremeau et al., 2001; Miyazaki et al., 2003). In addition, many nonprincipal cells were also labeled for VGLUT1 mRNA (Fig. 1A,C–E), including numerous neurons in the hilus of the dentate gyrus with a large cell body (Fig. 1A,E) that likely correspond to hilar mossy cells (Amaral, 1978; Soriano and Frotscher, 1994; Buckmaster et al., 1996; Liu et al., 1996; Wenzel et al., 1997) and a few neurons distributed within the dendritic layers of CA1–CA3. These latter neurons that were located mainly in the stratum lucidum of CA3 (Fig. 1C) and stratum radiatum of CA1 (Fig. 1D) likely correspond to, respectively, spiny nonpyramidal neurons (Soriano and Frotscher, 1993) and giant cells (Maccaferri and McBain, 1996; Gulyas et al, 1998).

The patterns of labeling were different in all pilocarpine-treated animals (n = 21/21) at all time intervals examined compared with control rats (Fig. 2). These differences were characterized mainly by a marked decrease in the number of VGLUT1 mRNA-containing neurons in the hilus of the dentate gyrus (Fig. 2C–H). These data are consistent with the death of mossy cells, as previously suggested (Obenaus et al., 1993; Buckmaster et al., 2002; Ferhat et al., 2003). This hilar cell loss contrasted with the good preservation of VGLUT1 mRNA-containing dentate granule cells and CA1–CA3 pyramidal cells (Fig. 2C–H) as well as VGLUT1 mRNA-labeled nonprincipal cells present in the CA1–CA3 dendritic layers (data not shown).

Surviving VGLUT1 mRNA-containing neurons (i.e., mostly principal neurons) in the hippocampal formation of pilocarpine-treated rats did not exhibit marked differences in the levels of VGLUT1 mRNA labeling intensity (Fig. 2C–H) compared with the levels in control animals (Fig. 2A,B) at any color-reaction times examined [2 hours (data not shown) and 5.5 hours (Fig. 2)]. Note that hilar ectopic granule cells that have been described in pilocarpine-treated animals (Parent et al., 1997, 2006; Scharfman et al., 2000; McCloskey et al., 2006) did not seem to display VGLUT1 mRNA.

Changes in VGLUT1 immunolabeling in the hippocampus of pilocarpine-treated rats

In control animals (n = 8/8), the immunolabeling for VGLUT1 was restricted mainly to axon terminals of glutamatergic neurons, as reported previously for the hippocampal formation of adult rats (Bellocchio et al., 1998; Fremeau et al., 2001; Kaneko et al., 2002). Briefly, the immunolabeling for VGLUT1 was characterized by diffuse labeling distributed in the stratum oriens and stratum radiatum of the CA1–CA3 area of the hippocampus, in the molecular layer and in the hilus of the dendate gyrus, and stratum lucidum (Fig. 3A). At higher magnification, this labeling correspond to punctiform structures in the molecular layer and in the hilus of the dentate gyrus (Fig. 3B).The labeling in CA1–CA3 neuropil corresponds to the axon terminals of CA3 pyramidal cells, the Schaffer collaterals. The labeling in the outer two-thirds of the dentate molecular layer corresponds to the terminals of the lateral and medial perforant path. The labeling in the inner one-third represents primarily staining of the axon terminals from the mossy cells located in the dentate hilus. The labeling in the hilus and stratum lucidum corresponds mainly to mossy fiber terminals. No to very low levels of labeling for VGLUT1 were observed in the pyramidal cell layer of the hippocampus and the granule cell layer of the dentate gyrus as well as in stratum lacunosum-moleculare of CA1 (Fig. 3).

The pattern of labeling for VGLUT1 was different in all pilocarpine-treated animals (n = 21/21) at all time intervals examined compared with that observed in control rats. One (n = 6/6) and two weeks (n = 6/6) after pilocarpine injection, the main difference compared with control animals was observed in the molecular layer of the dentate gyrus, consisting primarily of a massive decrease

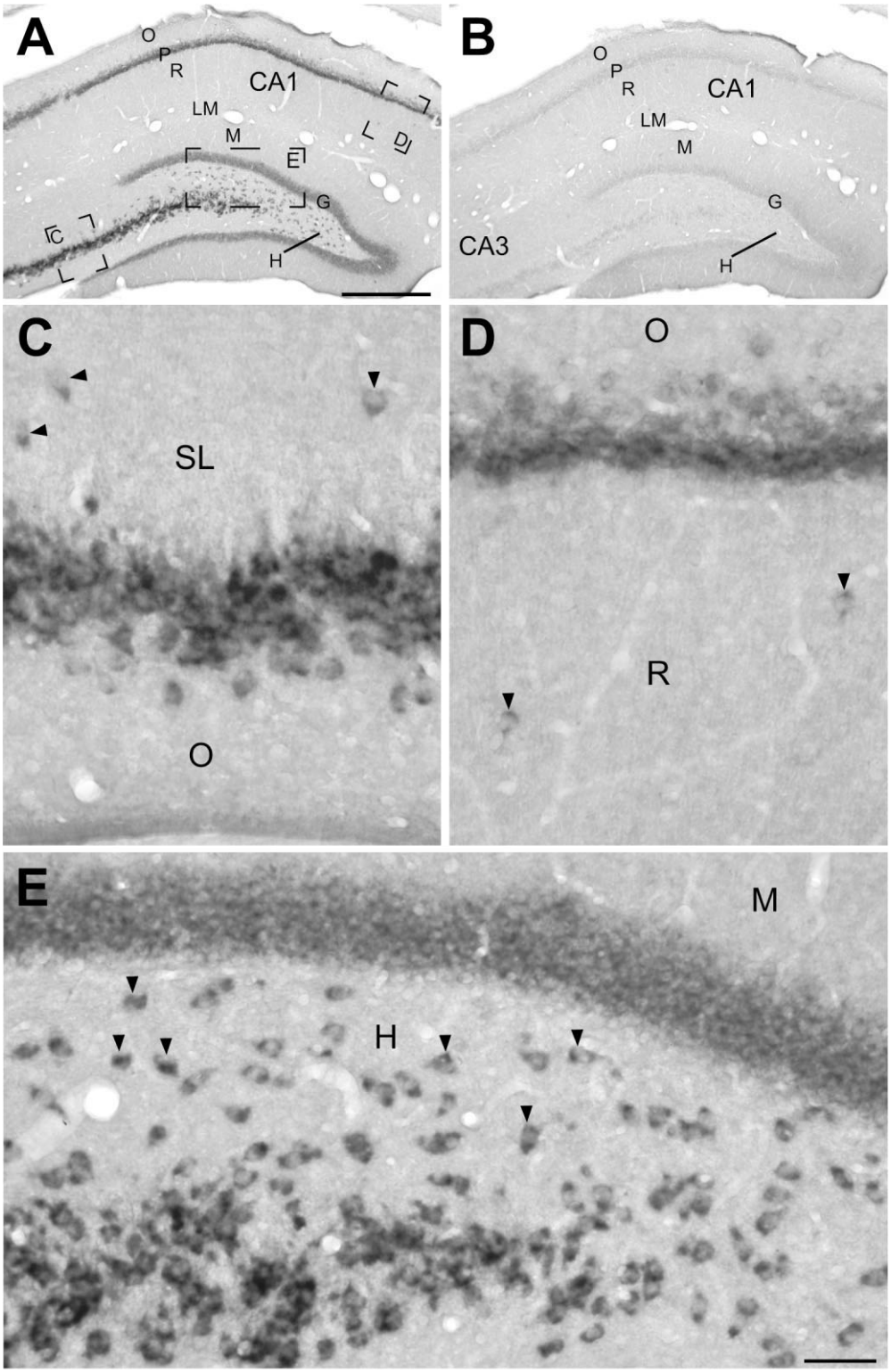

Fig. 1. Distribution of VGLUT1 mRNA-containing neurons in coronal sections of the rat hippocampal formation. **A:** In a section processed with antisense RNA probe, VGLUT1 mRNA is expressed in all glutamatergic neurons of the hippocampal formation, including the pyramidal cells (P) of CA1–CA3 regions, the granule cells (G) of dentate gyrus, and mossy cells of the hilus (H). **B:** In a section processed with sense RNA probe, faint nonspecific staining is observed in the cell body layers of the hippocampus and dentate gyrus. C–E: Higher magnifications of the CA3 (C), CA1 (D), and hilar (E) regions of the section illustrated in A. **C:** The size and shape of VGLUT1 mRNA-containing pyramidal cells and of neurons (arrowheads) distributed in the stratum lucidum (SL) of CA3 are evident. **D:** In CA1, some VGLUT1 mRNA containing neurons (arrowheads) are present in the stratum radiatum and likely correspond to glutamatergic giant cells. **E:** Numerous large and triangular VGLUT1 mRNA-containing cell bodies (arrowheads) are present in the hilus of the dentate gyrus. These neurons likely correspond to glutamatergic hilar mossy cells. LM, stratum lacunosum-moleculare; M, stratum moleculare; O, stratum oriens; R, stratum radiatum. Scale bars = 500 μm in A (applies to A,B); 50 μm in E (applies to C–E).

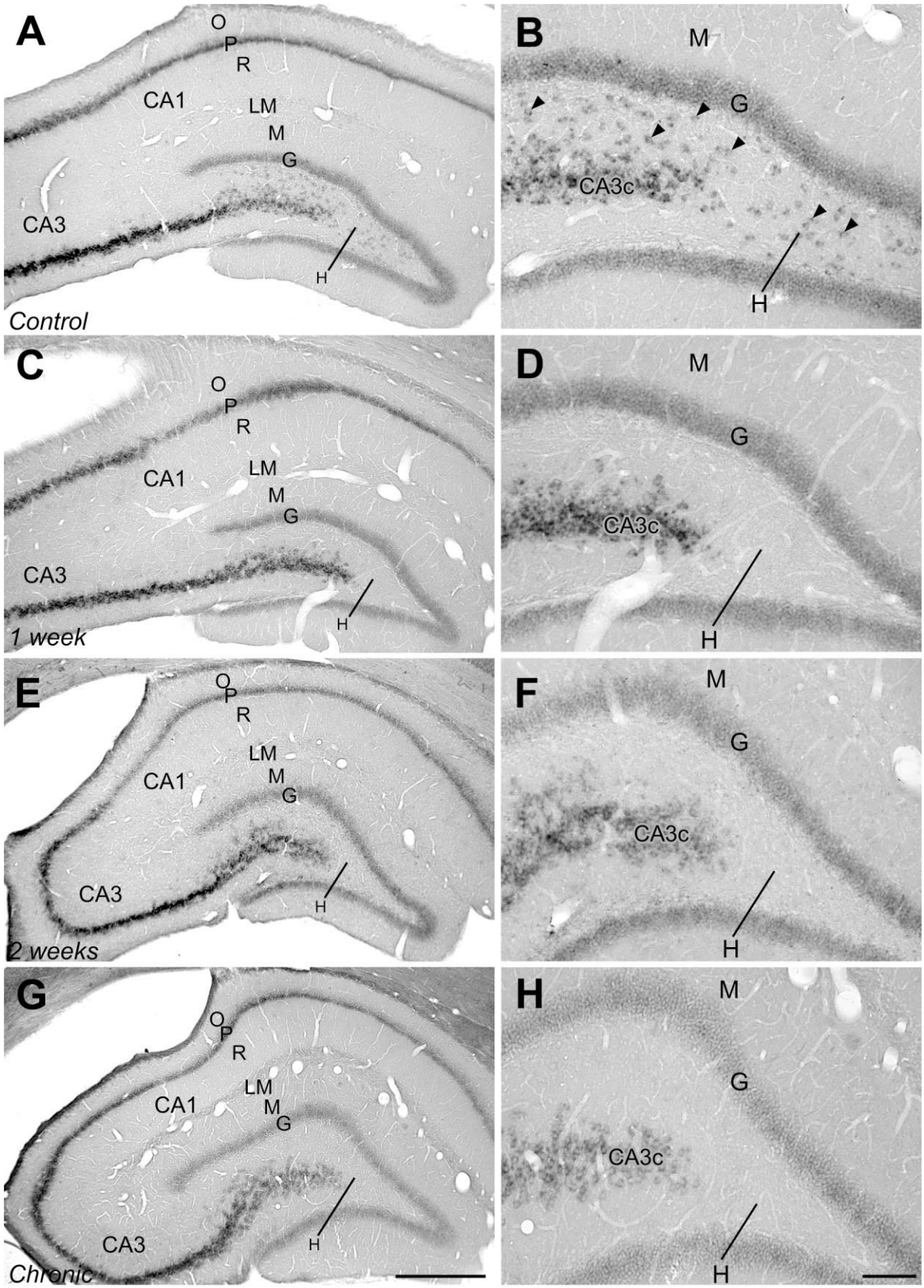

Fig. 2. Comparison of labeling for VGLUT1 mRNA in coronal sections of the hippocampal formation from control (**A,B**) and pilocarpine-treated rats at 1 week (**C,D**), 2 weeks (**E,F**), and 12 weeks (**G,H**) processed for the same color reaction time. A,B: In a section from a control rat, the pyramidal cell of CA1–CA3 region of the hippocampus and granule cells and hilar mossy cells of the dentate gyrus exhibit moderate to strong levels of labeling for VGLUT1 mRNA. C–H: In all sections from pilocarpine-treated animals at 1 week (C,D) 2 weeks (E,F) and chronic stage (G,H), a marked decrease in the number of VGLUT1-containing mossy cells is observed in the hilus (H) of the dentate gyrus. The levels of labeling in the pyramidal cell (P) and granule cell (G) layers are similar to the levels observed in control animals (compare C–H to A,B). LM, stratum lacunosum-moleculare; M, stratum moleculare; O, stratum oriens; R, stratum radiatum. Scale bars = 500 μm in G (applies to A,C,E,G); 125 μm in H (applies to B,D,F,H).

in the labeling intensity in the inner one-third of the molecular layer (compare Fig. 3C–F with Fig. 3A,B). The loss of labeling in this region contrasted with the preservation of the labeling in the outer two-thirds of the molecular layer. The overall laminar patterns of labeling for VGLUT1 in the hilus of the dentate gyrus and in the hippocampus were similar in control animals and in pilocarpine-treated animals at both 1 and 2 weeks (compare Fig. 3C–F with Fig. 3A,B). In some animals (1 week, n = 3/6; 2 weeks, n = 4/6), an increase in the labeling intensity was observed in the stratum lucidum, the mossy fiber pathway (compare Fig. 3C,E with Fig. 3A).

The pattern of staining for VGLUT1 in all chronic pilocarpine-treated animals (Fig. 3G,H) differed from that found in pilocarpine-treated animals at 1 (Fig. 3C,D) and 2 (Fig. 3E,F) weeks and in control rats (Fig. 3A,B). All chronic pilocarpine-treated animals (from 8 to 16 weeks after pilocarpine injection, n = 9) displayed in contrast to pilocarpine-treated rats at 1 and 2 weeks and control animals a much higher level of labeling in the inner one-third of the molecular layer than that in the outer two-thirds (Fig. 3G,H). This level of staining appeared higher than that observed in the inner molecular layer of control animals (Fig. 3B) and contrasted with the almost complete loss of labeling observed in pilocarpine-treated rats at 1 and 2 weeks (Fig. 3D,F). In the chronic pilocarpine-treated animals, mossy-fiber-like terminals were present in this inner one-third of the molecular layer (Fig. 3H).

In addition to this distinct change in the pattern of labeling in the molecular layer of the dentate gyrus, a strong increase in the labeling intensity was consistently observed in the stratum lucidum and all dendritic layers of the CA1–CA3 hippocampal regions in chronic pilocarpine-treated rats (Fig. 3G; n = 9/9). The increased level of labeling intensity in the CA1–CA3 dendritic layers was not observed in pilocarpine-treated animals at 1 and 2 weeks (Fig. 3C,E).

Changes in VGAT mRNA labeling in the hippocampus of pilocarpine-treated rats

In control animals (n = 8/8), when sections were incubated for optimal color-reaction time (47 hours), neurons labeled for VGAT mRNA were distributed through all layers of the hippocampal formation (Fig. 4B), as previously reported (McIntire et al., 1997; Sagné et al., 1997). Such a pattern was very similar to that of GAD mRNA-containing neurons in the hippocampus (Houser and Esclapez, 1994; Esclapez and Houser, 1999). The pyramidal cell and dentate granule cell layers displayed a low level of nonspecific staining (Fig. 4B), since similar labeling was observed with sense control probe (compared Fig. 4B with Fig. 4A).

After optimal color-reaction time (26 hours), the patterns of labeling were different in all pilocarpine-treated animals (n = 21/21) at all time intervals examined (Figs. 4C,D, 5B–D) compared with that observed in control rats (Fig. 4B). A marked decrease in the number of VGAT mRNA-containing neurons was observed in the hilus of the dentate gyrus (compare Fig. 4B with Figs. 4C,D, 5B–D). This finding is consistent with the cell death of GAD-containing neurons, previously demonstrated by Obenaus et al. (1993) in this model.

In addition, all pilocarpine-treated animals exhibited marked differences in the intensity of labeling for VGAT mRNA compared with control animals, when sections were incubated for the same color-reaction times. Such increases were quite prominent, and the clearest indication of these increases was provided when sections were processed for a shorter time (20 hours) in the chromogen solution (Fig. 5). In sections from control animals, VGAT mRNA-containing neurons were detected within the hippocampal formation, but these neurons were only lightly labeled for VGAT mRNA (Fig. 5A). In sections from pilocarpine-treated rats, surviving VGAT mRNA-containing neurons within the hippocampal formation, including those along the inner border of the granule cell layer and the remaining neurons in the deep hilus, were labeled distinctly, and virtually all of these neurons exhibited a strong level of labeling (Fig. 5B–D).

After longer color-reaction times (40 hours), differences in the levels of labeling among sections from pilocarpine-treated and control rats also were observed (compare Fig. 6A with Fig. 6B–D). However, these differences were less marked than when sections were processed for a shorter time in the chromogen solution. In sections from control rats, after the longer incubation time, virtually all labeled neurons in the hippocampus and dentate gyrus displayed an intense reaction product for VGAT mRNA (Fig. 6A), and this level of labeling clearly was higher than that in sections processed for only 20 hours in the chromogen solution (compare Fig. 6A with Fig. 5A). In sections from all pilocarpine-treated animals, the entire population of labeled neurons within the hippocampal formation exhibited very strong levels of labeling for VGAT mRNA (Fig. 6B–D). The intensities of labeling of VGAT mRNA-containing neurons were higher than those observed at shorter (20 hours) color-reaction times (compare Fig. 6B–D with Fig. 5B–D). Despite the strong labeling observed in all sections, labeling intensities of VGAT mRNA-containing neurons in control animals were lower than those in pilocarpine-treated animals (compare Fig. 6A with Fig. 6B–D).

Increases in immunohistochemical labeling for VGAT in pilocarpine-treated rats

In control animals (n = 8/8), VGAT immunolabeling was present in all layers of the hippocampal formation (Fig. 7A,B), in agreement with previous reports (Chaudhry et al., 1998). This labeling corresponds to axon terminals of GABAergic interneurons (Chaudhry et al., 1998) and was concentrated most highly within the pyramidal cell layer of the hippocampus and in the outer part of the granule cell layer of the dentate gyrus (Fig. 7B). Furthermore, extensive fields of VGAT-containing terminals were observed within the dendritic layers of the hippocampal formation. High densities of VGAT immunolabeling were present in the outer one-third of the molecular layer of the dentate gyrus and at the border between the stratum lacunosum-moleculare and the stratum radiatum of the hippocampus, whereas lower densities of VGAT immunolabeling were observed in the other layers (Fig. 7A,B). In the hippocampal formation, the pattern of distribution for VGAT-containing terminals is similar to that of GAD65- and GAD67-containing terminals (Houser and Esclapez, 1996; Esclapez and Houser, 1999), except for the mossy fibers terminals, which were labeled for GAD67 (Schwarzer and Sperk, 1995; Sloviter et al., 1996) but not for GAD65 (Houser and Esclapez, 1996; Esclapez and Houser, 1999) and not for VGAT (Chaudhry et al., 1998; Sperk et al., 2003) as reported previously.

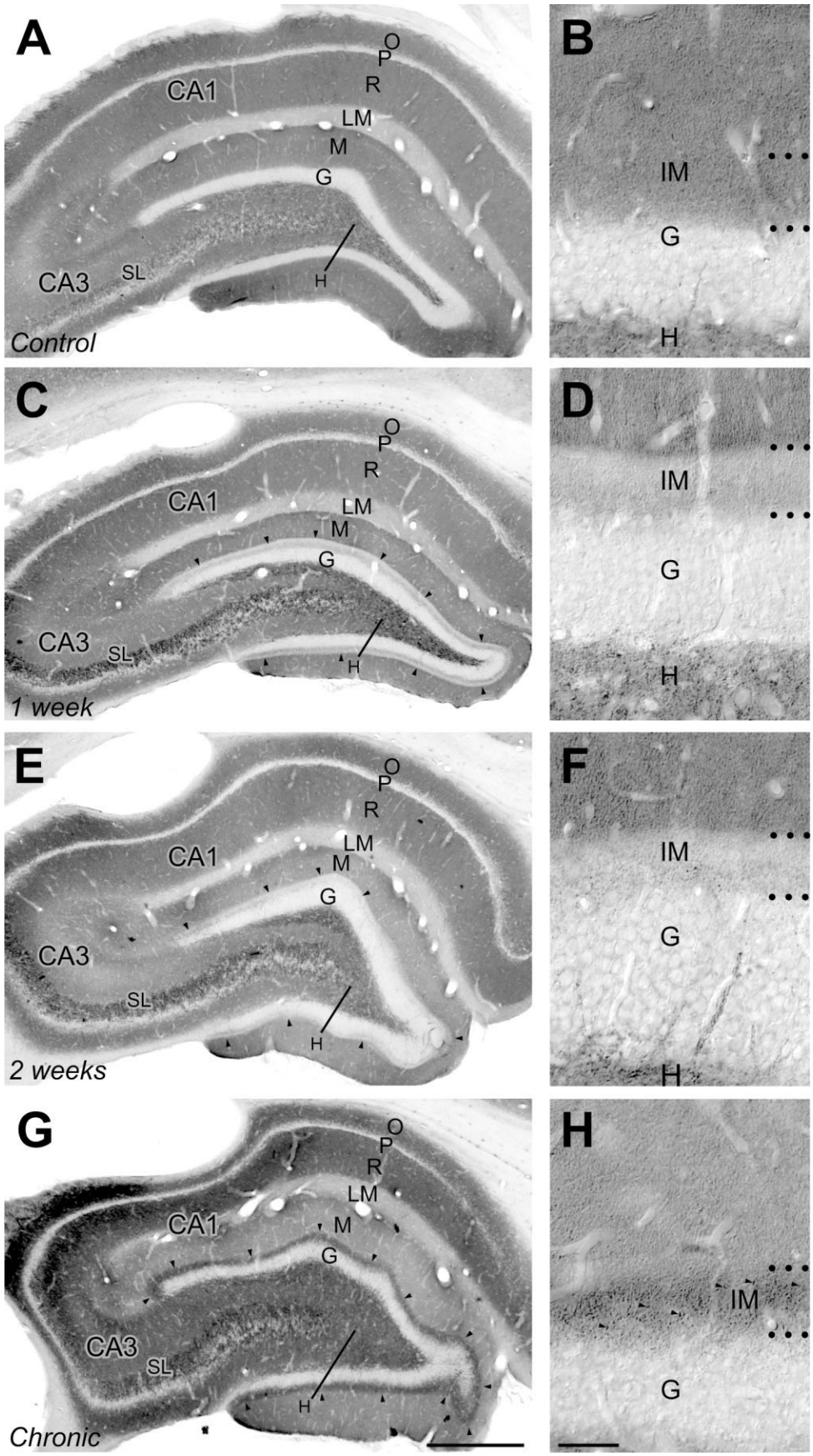
A
O
P
R
LM
M
G
CA1
CA3
SL
H
Control
B
IM
G
H
C
O
P
R
CA1
LM
M
G
CA3
SL
H
1 week
D
IM
G
H
E
O
P
R
LM
M
G
CA1
CA3
SL
H
2 weeks
F
IM
G
H
G
O
P
R
LM
M
G
CA1
CA3
SL
H
Chronic
H
IM
G

Figure 3

In all pilocarpine-treated rats at 1 week (n = 6/6) and 2 weeks (n = 6/6), a clear increase in the labeling of VGAT-containing axon terminals was observed in virtually all regions of the hippocampal formation (Fig. 7C–E). The increased labeling was particularly striking in the stratum lacunosum-moleculare and in the inner one-third of the molecular layer of the dentate gyrus. In this inner part of the molecular layer, the levels of labeling were increased to a much greater extent than in the middle part of the molecular layer (Fig. 7C–F). Except for differences in the levels of immunoreactivity, the overall laminar patterns of labeling for VGAT-containing terminals were similar in pilocarpine-treated at 1 and 2 weeks and in control rats.

The labeling for VGAT in all chronic pilocarpine-treated animals (n = 9/9; Fig. 7G,H) differed from that found in pilocarpine-treated animals at 1 and 2 weeks (Fig. 7C,F) and in control rats (Fig. 7A,B). Chronic pilocarpine-treated animals displayed a much higher level of labeling in all layers of the hippocampus and dentate gyrus than did pilocarpine-treated rats at 1 and 2 weeks (Fig. 7C,E,G) or control animals (Fig. 7A). In addition, the laminar pattern of labeling in the molecular layer of the dendate gyrus in chronic pilocarpine-treated animals (Fig. 7G,H) differed strongly from the patterns observed in pilocarpine-treated rats at 1 (Fig. 7C,D) and 2 weeks (Fig. 7E,F) and in control rats (Fig. 7A,B). In chronic pilocarpine animals, the level of labeling in the outer two-thirds of the molecular layer was comparable to that in the inner one-third (Fig. 7C,D).

Simultaneous detection of VGLUT1, VGAT, and GAD65

For pilocarpine-treated animal, we reported increased immunohistochemical labeling for VGLUT1 and VGAT in the inner molecular layer of the dentate gyrus. To determine whether such an increase involved the same or different populations of terminals, we performed simultaneous detection of the two transporters. In all chronic pilocarpine-treated animals (n = 9/9), numerous VGLUT1-labeled terminals were observed in the inner molecular layer of the dentate gyrus (Fig. 8A,D) but none of them contained VGAT (Fig. 8B,D) or GAD65 (Fig. 8C,D). Virtually, all VGAT-labeled terminals coexpressed GAD65, including terminals surrounding granule cells somata (Fig. 8B–D).

Fig. 3. Comparison of immunohistochemical labeling for VGLUT1 in coronal sections of the hippocampal formation from control (**A,B**) and pilocarpine-treated animals at 1 week (**C,D**), 2 weeks (**E,F**), and 12 weeks (**G,H**). A,B: In a control rat, immunolabeling for VGLUT1, which is concentrated in axon terminals of the intrinsic glutamatergic network, includes fine punctiform structures distributed uniformly in the stratum oriens (O) and stratum radiatum (R) of the CA1–CA3 area of the hippocampus and in the molecular layer (M) of the dendate gyrus (DG), as well as in the hilus (H) and stratum lucidum (SL). C–F: In pilocarpine-treated rats at 1 (C,D) and 2 weeks (E,F), VGLUT1 immunoreactivity is strongly decreased in the inner zone of the molecular layer (IM), whereas the pattern and intensity of labeling in the other hippocampal layers are similar to those of a control rat. G,H: In pilocarpine-treated rats at 12 weeks, VGLUT1 immunoreactivity is increased in the IM of the DG, concentrated in terminal-like structures (arrowheads), compared with control (A,B) animals and pilocarpine-treated rats at 1 (C,D) and 2 weeks (E,F). Such terminals likely represent mossy fiber terminals known to establish aberrant connections in this region. An increased VGLUT1 immunoreactivity is observed in the dendritic layers of CA1–CA3 hippocampal region. Such an increase could represent sprouting of pyramidal cell axons. G, granule cell layer; H, hilus of dentate gyrus; IM, inner molecular layer; LM, stratum lacunosum-moleculare; M, stratum moleculare; O, stratum oriens; P, stratum pyramidale; R, stratum radiatum. Scale bars = 500 μm in G (applies to A,C,E,G); 50 μm in H (applies to B,D,F,H).

DISCUSSION

This study demonstrates that, during epileptogenesis induced by pilocarpine, the intrinsic glutamatergic and GABAergic neuronal networks differ with respect to the type and the time course of their reorganizations. The reorganization of surviving GABAergic neurons is characterized mainly by an up-regulation of VGAT at the mRNA and protein levels, which likely reflects an increased presynaptic activity. This presynaptic plasticity of the GABAergic neurotransmission occurs as early as the beginning of the latent period and persists during the chronic stage. The reorganization of the glutamatergic principal neurons is characterized by an increase of VGLUT1-containing terminals that corresponds mainly to axonal sprouting and aberrant synaptogenesis. This structural reorganization occurred at the chronic stage. Furthermore, our data strongly support and confirm cell death of vulnerable subpopulations of glutamatergic and GABAergic neurons. Death of both types of neuron occurs during the latent period.

Methodological considerations

Our data demonstrate that, within the hippocampal formation, the intensities of labeling for VGAT mRNA-containing neurons were consistently stronger in pilocarpine-treated rats than in control animals. We view these findings as an indication of increased levels of VGAT mRNAs in the hippocampal GABA neurons of pilocarpine-treated rats. This interpretation is consistent with previous biochemical studies, which have shown that differences in the intensity of labeling with nonradioactive hybridization methods reflect differences in the relative amounts of mRNA among neurons, just as different concentrations of silver grains, when using radioactive methods, indicate different amounts of mRNA (Hoëltke and Kessler, 1990; Esclapez et al., 1993, Esclapez and Houser, 1999). Such differences between control and pilocarpine-treated animals are not observed with VGLUT1 mRNA. These findings argue against the suggestion that differences in labeling intensities between the control and the pilocarpine-treated rats, observed for VGAT mRNA, reflect variability of labeling resulting from differences in tissue properties. They further support that differences in neuronal labeling observed with nonradioactive in situ hybridization among sections from control and pilocarpine-treated rats reflect differences in relative level of mRNA. However, as previously discussed (Esclapez and Houser, 1999), because the enzymatic and immunohistochemical methods for mRNA detection are not linear reactions, relative levels of mRNA can not be related directly to absolute concentrations of mRNA without confirmation with isotopic methods. Nevertheless, the present study confirms that nonradioactive in situ hybridization technique can be use to estimate differences in relative level of mRNA.

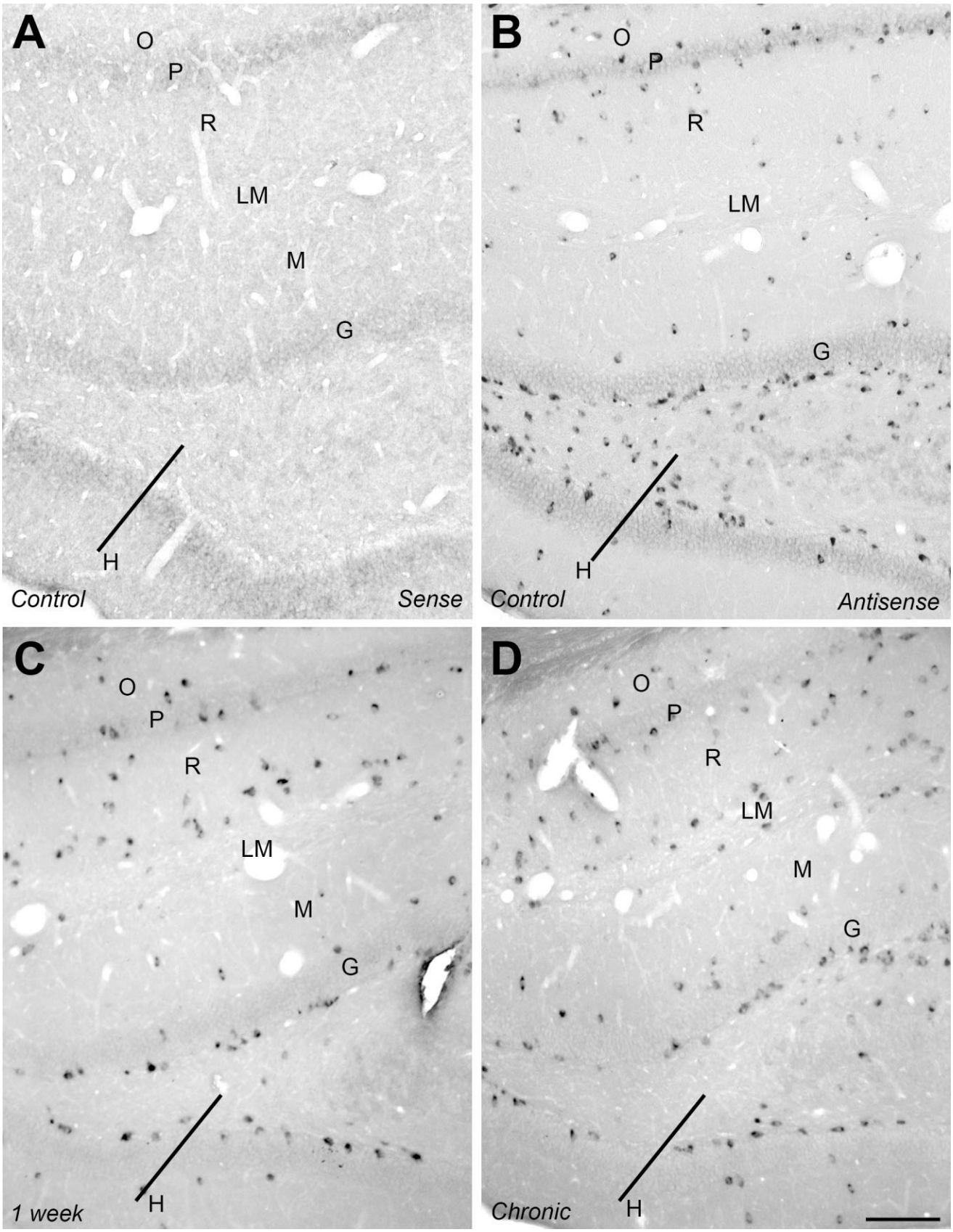
A
O
P
R
LM
M
G
H
Control
Sense
B
O
P
R
LM
G
H
Control
Antisense
C
O
P
R
LM
M
G
H
1 week
D
O
P
R
LM
M
G
H
Chronic

Figure 4

VGLUT1, a marker of vulnerability and reorganization of the intrinsic hippocampal glutamatergic network during development of pilocarpine-induced epilepsy

For the pilocarpine model of temporal lobe epilepsy, we report a striking decrease of VGLUT1 mRNA-containing cell bodies in the hilus of the dentate gyrus during the latent period, which persists during the chronic stage. Such a decrease is associated with a loss of VGLUT1-containing terminals in the inner one-third of the molecular layer of the dentate gyrus, clearly observed during the latent period (1 and 2 weeks after pilocarpine injection). In the hippocampal formation, VGLUT1 is expressed specifically in the glutamatergic neurons and their axon terminals (Bellocchio et al., 1998; Fremeau et al., 2001). Therefore, our results for VGLUT1 in pilocarpine-treated animals clearly demonstrate the loss of a population of glutamatergic hilar neurons, the axons of which project in the inner one-third of the molecular layer, i.e., the mossy cells (Soriano and Frotscher, 1994). This cell loss that occurred after the status epilepticus likely corresponds to the neuronal death of these neurons, insofar as it is still observed several months later. Indeed, mossy cells have been considered to be, with hilar GABAergic neurons, the first neuronal populations to die in experimental models of temporal lobe epilepsy (Nadler et al., 1980; Sloviter and Nilaver, 1987; Cavazos and Sutula, 1990; Sloviter et al., 2003), including the pilocarpine model (Obenaus et al., 1993; Houser and Esclapez, 1996; Buckmaster et al., 2002; Ferhat et al., 2003). The notion of their vulnerability is based on studies showing 1) degenerating axon terminals in the inner molecular layer (Obenaus et al., 1993), 2) loss of synaptophysin-containing terminals in the inner molecular layer (Ferhat et al., 2003), 3) degenerating cell bodies in the hilus of the dentate gyrus (Obenaus et al., 1993; Dinocourt et al., 2003), and 4) loss of glutamate receptor-2-labeled cell bodies in the hilus (Sloviter et al., 2003). However, these markers are not specific for mossy cells or glutamatergic neurons and their axon terminals. The concept of highly vulnerable mossy cells has been questioned based on intracellular recordings of remaining mossy cells after pilocarpine-induced seizures (Scharfman et al., 2001; for review see Sloviter et al., 2003). Our data directly establish that glutamatergic mossy cells degenerate in the pilocarpine-treated rat and that such neuronal death occurs at the beginning of the latent period, in parallel with the neuronal loss of hilar GABAergic cells. Vulnerability of hilar GABAergic neurons, first demonstrated in this model by Obenaus et al. (1993), is confirmed in this study by the marked loss in the number of VGAT mRNA-containing hilar neurons that occurs after status epilepticus and persists 16 weeks later.

The subsequent overshooting recovery of VGLUT1 immunoreactivity in the inner molecular layer of the dentate gyrus, starting 2 weeks after pilocarpine injection and massive at the chronic stage, likely is due to the progressive sprouting of mossy fibers, the axons of glutamatergic granule cells. This hypothesis is supported by the glutamatergic properties of these terminals, which were not labeled for VGAT and GAD65. Such sprouting has been extensively described in experimental model of temporal lobe epilepsy (Cronin and Dudek, 1988; Represa et al., 1993; Buckmaster and Dudek, 1997; Sutula et al., 1998; Wenzel et al., 2000), including in the pilocarpine model (Mello et al., 1993; Okazaki et al., 1995; Buckmaster et al., 2002), and is thought to result in the establishment of functional excitatory synaptic boutons on granule cell dendrites (Wuarin and Dudek, 1996, 2001; Molnar and Nadler, 1999; Lynch and Sutula, 2000; Buckmaster et al., 2002; Scharfman et al., 2003).

It has been hypothesized that mossy cell death, and the consequent loss of its projections to the inner molecular layer, would vacate synaptic contacts on granule cell dendrites and interneurons and thus trigger inappropriate sprouting of mossy fibers into that region (Cavazos and Sutula, 1990; Houser et al., 1990; Babb et al., 1991; Masukawa et al., 1997). The temporal profile of changes for VGLUT1-containing terminals in the inner molecular layer during the development of pilocarpine-induced epilepsy supports such a hypothesis.

In addition to the vulnerability of mossy cells and reorganization of mossy fibers, illustrated by loss and regain of VGLUT1 immunoreactivity in the inner molecular layer, our data show an increase in the immunoreactivity of VGLUT1-containing terminals in all dendritic layers of the CA1–CA3 hippocampal regions in chronic pilocarpine-treated animals. Such an increase is not present in pilocarpine-treated animals at 1 and 2 weeks. The increased levels of immunoreactivity at the chronic stage presumably reflect increased levels of VGLUT1 protein in the terminals. However, the observed increase is not associated with an up-regulation of VGLUT1 mRNA and thus may not correspond to a substantial increase in the production of VGLUT1. A more likely alternative explanation for such increased levels of VGLUT1 immunoreactivity in the hippocampus of pilocarpine-treated animals is an increase in the density (number) of VGLUT1-containing terminals. Indeed, an axonal sprouting of CA1–CA3 pyramidal cells has been described in the chronic pilocarpine-treated animals (Esclapez et al., 1999; Lehmann et al., 2001), and these newly formed glutamatergic nerve endings are functional (Esclapez et al., 1999).

Therefore, the increased levels of VGLUT1 immunoreactivity strongly reflect the reorganization of the glutamatergic principal neurons characterized by the sprouting of glutamatergic fibers and associated neosynaptogenesis. Furthermore, our results demonstrate that such axonal

Fig. 4. Distribution of VGAT mRNA-containing neurons in coronal sections of the rat hippocampus from control and chronic pilocarpine-treated rats processed for optimal color reaction times. **A:** In a section processed with sense RNA probe and developed 47 hours in the chromogen reaction, only faint, nonspecific staining is observed in the pyramidal and granule cell layers (G). **B:** In a section of a control rat processed with antisense RNA probe and developed 47 hours in the chromogen reaction, VGAT mRNA-containing cell bodies are distributed in all layers of the dentate gyrus and of the hippocampus. Many labeled neurons are evident throughout the stratum oriens (O), the pyramidal cell layer (P), the stratum radiatum (R), the molecular layer (M), and the hilus (H) of the dentate gyrus. **C,D:** In sections of a 1-week (C) and a chronic (D) pilocarpine-treated rat processed with antisense RNA probe and developed at 26 hours in the chromogen reaction, many VGAT mRNA-containing neurons are evident throughout all layers of the dentate gyrus and CA1–CA3. The number of VGAT mRNA-containing neurons in the hilus of the dentate gyrus is reduced compared with control animals (compare C with B). LM, stratum lacunosum-moleculare. Scale bar = 125 μm.

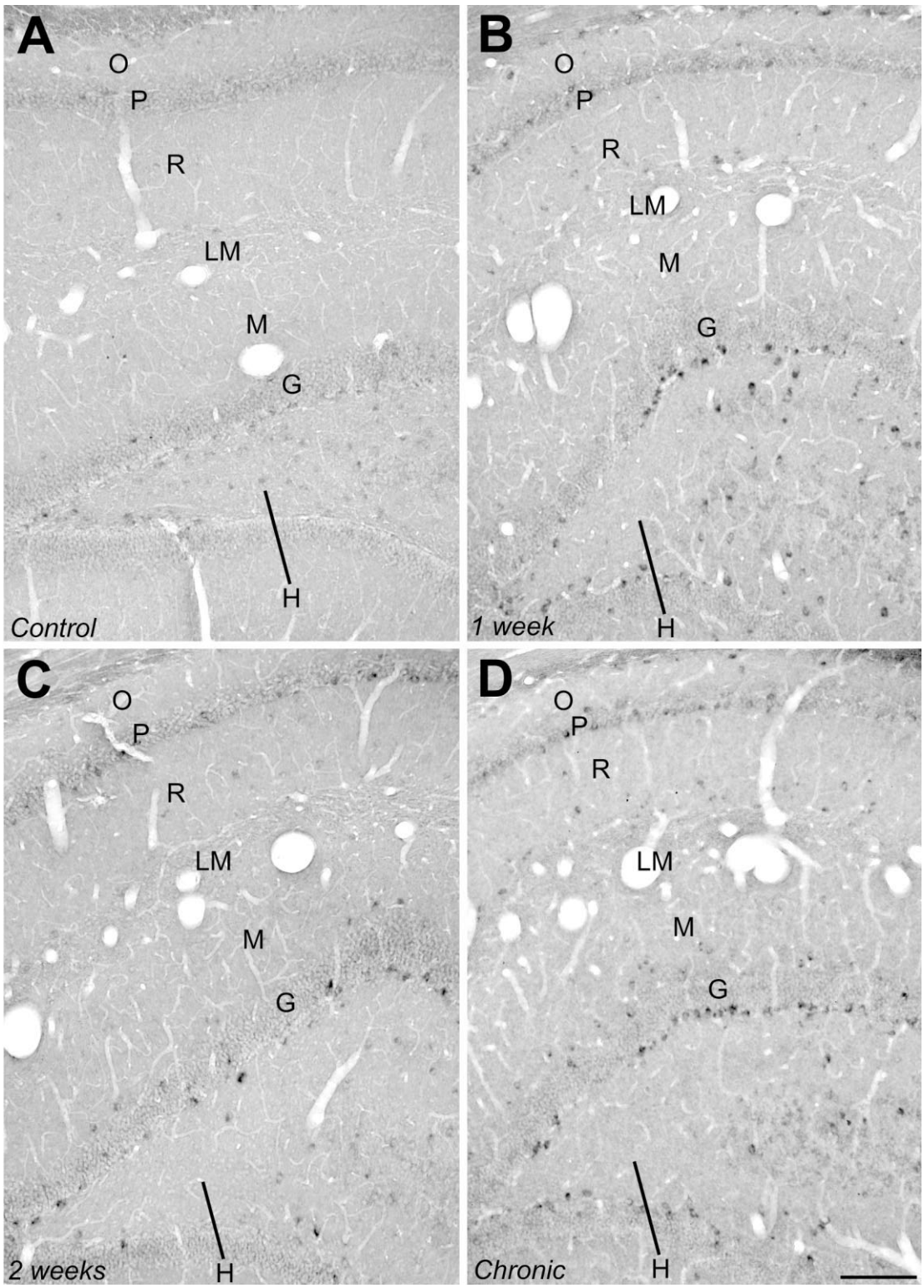

Fig. 5. Comparison of labeling for VGAT mRNA in coronal sections of the hippocampal formation from control (**A**) and pilocarpine-treated rats at 1 week (**B**), 2 weeks (**C**), and 12 weeks (**D**) processed for the same short color-reaction time (20 hours). A: Section from a control animal, processed for a short time in the chromogen solution. Under this condition, only very few and faintly labeled VGAT mRNA-containing interneuron cell bodies are detected in the hippocampus and dentate gyrus compared with sections processed for longer color-reaction time (compare with Figs. 4A, 6A). B–D: In sections from pilocarpine-treated rats, processed for the same short color-reaction time, many VGAT mRNA-containing neurons are evident throughout all layers of the dentate gyrus and CA1–CA3. These neurons exhibit moderate to strong levels of labeling for VGAT mRNA. Differences in the level of labeling are particularly striking between control animals and all pilocarpine-treated rats. Levels of labeling in pilocarpine-treated rats are clearly higher than those in control rats (compare B–D with A). G, granule cell layer; LM, stratum lacunosum-moleculare; M, stratum moleculare; O, stratum oriens; P, stratum pyramidale; R, stratum radiatum. Scale bar = 125 μm.

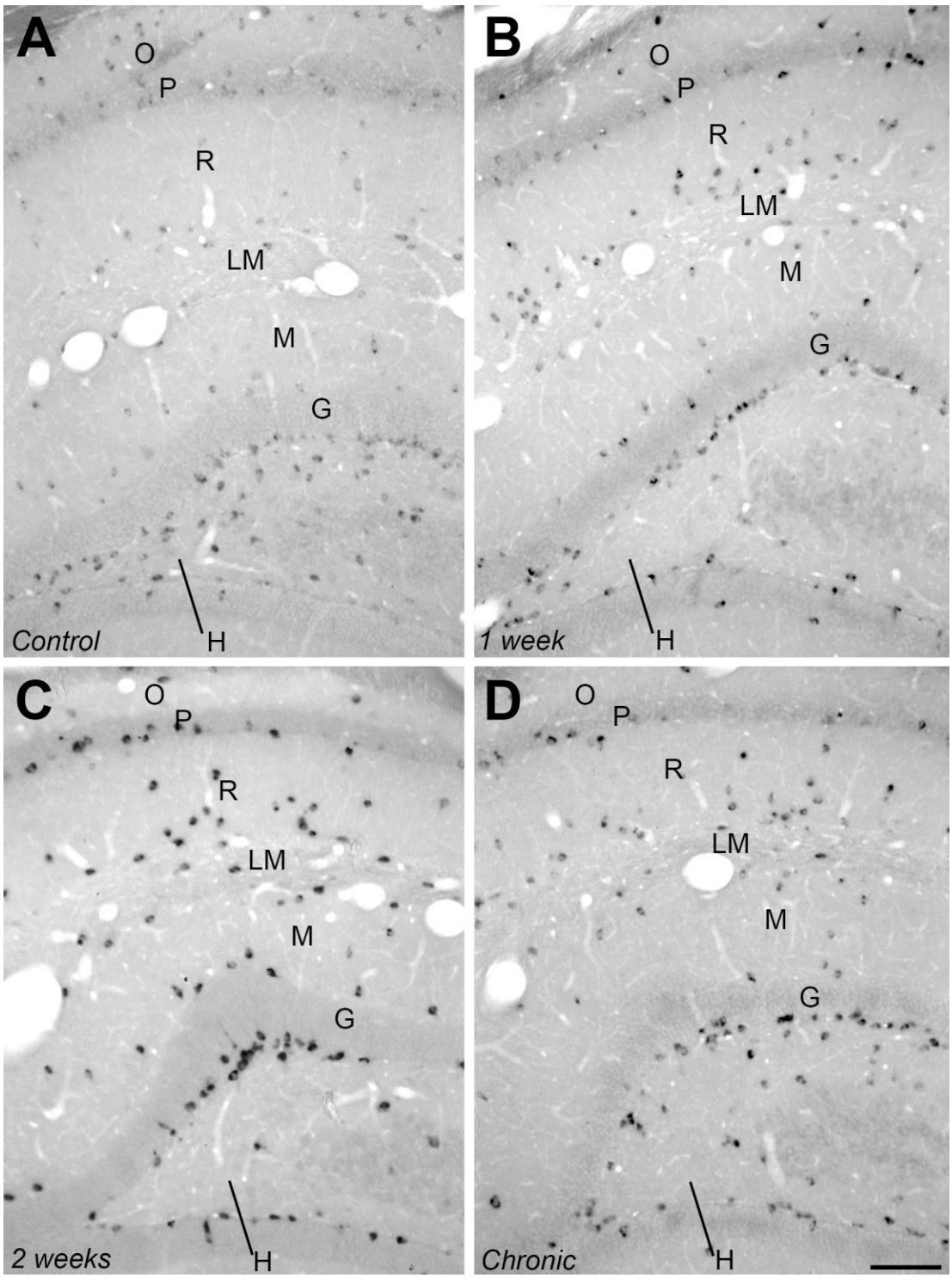

Fig. 6. Comparison of labeling for VGAT mRNA in coronal sections of the hippocampal formation from control (**A**) and pilocarpine-treated rats at 1 week (**B**), 2 weeks (**C**), and 12 weeks (**D**) processed for the same long color-reaction time (40 hours). A: In a section from a control rat processed for 40 hours, virtually all labeled neurons in the hippocampus and dentate gyrus display a strong reaction product for VGAT mRNA. This level of labeling clearly is higher than that in sections processed for 20 hours in the chromogen solution (compare with Fig. 5A). B–D: In sections from all pilocarpine-treated animals, the entire population of labeled neurons within the hippocampal formation exhibits very high levels of labeling for VGAT mRNA. The intensities of labeling of VGAT mRNA-containing neurons are higher than those observed at shorter (20 hours) color-reaction times (compare with Fig. 5B–D). Levels of labeling in pilocarpine-treated rats are still clearly higher than those in control rats (compare B–D with A). G, granule cell layer; LM, stratum lacunosum-moleculare; M, stratum moleculare; O, stratum oriens; P, stratum pyramidale; R, stratum radiatum. Scale bar = 125 μm.

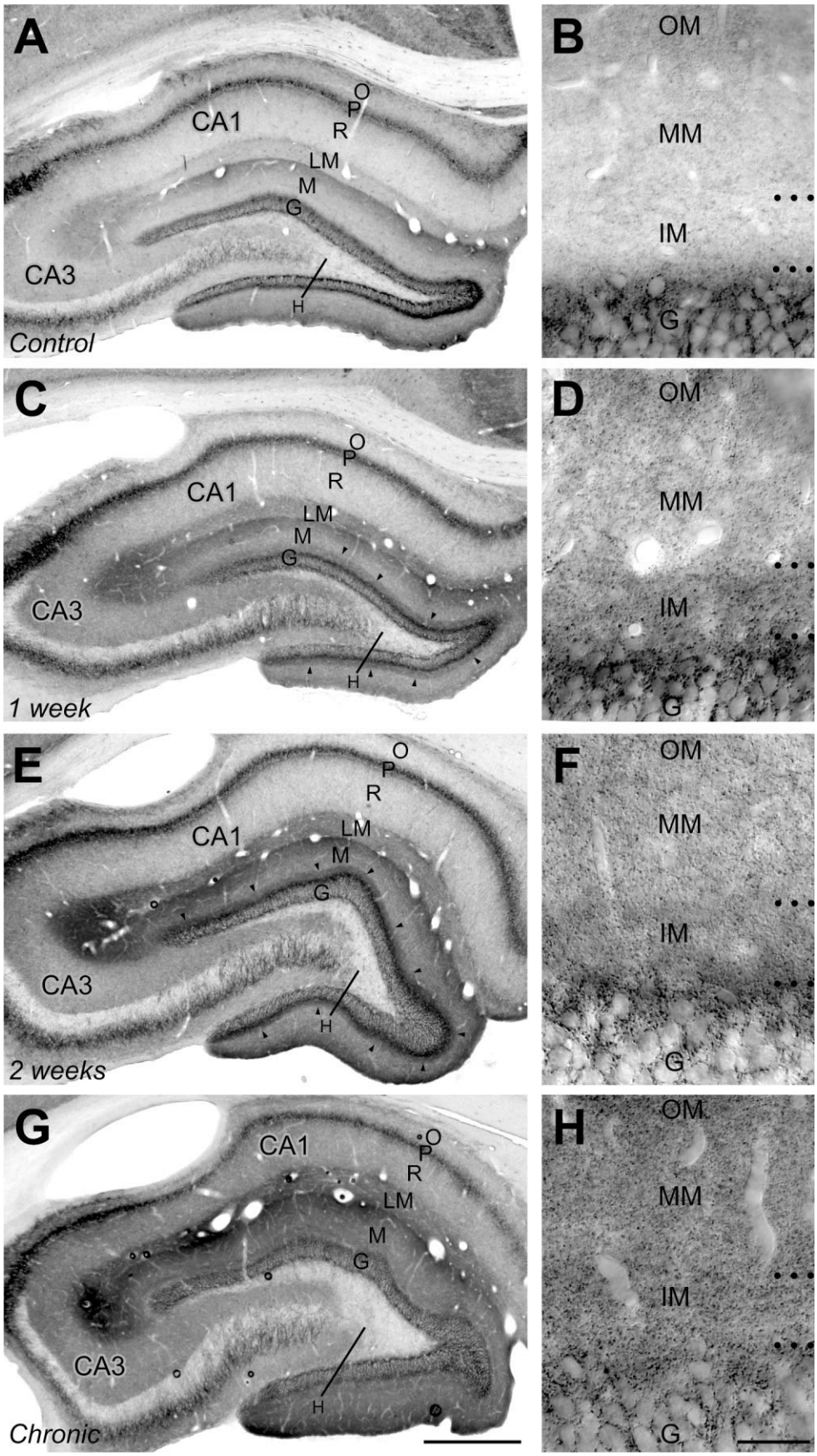
A
CA1
O
P
R
LM
M
G
CA3
H
Control
B
OM
MM
IM
G
C
CA1
CA3
1 week
D
E
CA1
CA3
2 weeks
F
G
CA1
CA3
Chronic
H

Figure 7

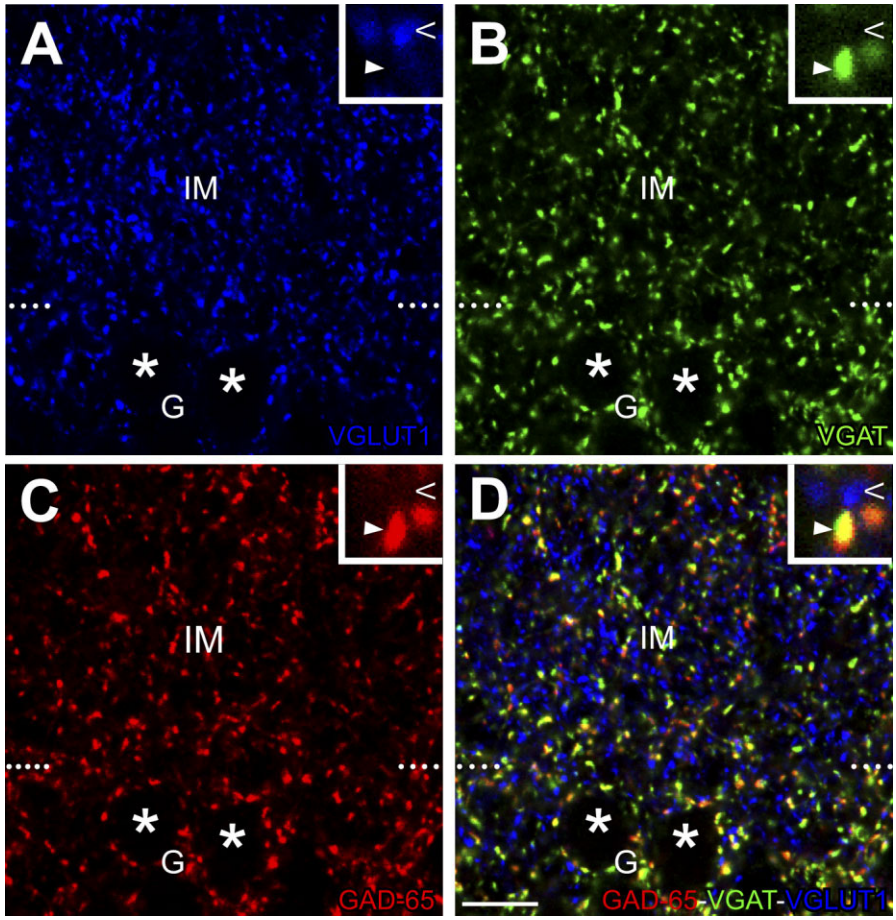

Fig. 8. Simultaneous detection of VGLUT1, VGAT, and GAD65 in the inner molecular layer of the dentate gyrus in a coronal section of a chronic pilocarpine-treated rat. **A:** In the chronic pilocarpine animal, numerous VGLUT1-containing terminals (blue) are present in the inner molecular layer (IM) of the dentate gyrus. **B,C:** Numerous VGAT-containing (B, green) and GAD65-containing (C, red) terminals are observed in the same region. **D:** Merge of VGLUT1 (blue), VGAT (green), and GAD65 (red). No colocalization between VGLUT1 and VGAT or VGLUT1 and GAD65 is detected (would be white). In contrast, virtually all VGAT-labeled terminals contain GAD65 (yellow-orange), including terminals surrounding the soma of granule cells (asterisks). *Insets* illustrate, at high magnification, a terminal singly labeled for VGLUT1 (open arrowhead) and a terminal doubly labeled for VGAT and GAD65 (solid arrowhead, yellow). Scale bar = 10 μm.

Fig. 7. Comparison of immunohistochemical labeling for VGAT in coronal sections of the hippocampal formation from control (**A,B**) and pilocarpine-treated animals at 1 week (**C,D**), 2 weeks (**E,F**), and 12 weeks (**G,H**). A,B: In a control rat, immunoreactivity for VGAT, which is concentrated in axon terminals of GABAergic neurons, is present in cell body layers as well as in all dendritic regions of the hippocampal formation. C–F: In pilocarpine-treated rats at 1 and 2 weeks, VGAT immunoreactivity is increased in all layers of the hippocampus, including the stratum oriens (O), stratum pyramidale (P), stratum radiatum (R), and stratum lacunosum-moleculare (LM), as well as in the molecular layer (M) of the dentate gyrus (DG). Labeling is increased to a greater extent in the inner molecular layer (arrowheads) than in the middle molecular layer (MM). G,H: In a pilocarpine-treated animal at 12 weeks, the levels of labeling in all layers of the hippocampus and dentate gyrus are higher than those in pilocarpine-treated rats at 1 week (C,D) and in control animals (A,B). The level of labeling in the outer two-thirds of the molecular layer is higher than that observed in pilocarpine-treated rats at 1 and 2 weeks. Scale bars = 500 μm in G (applies to A,C,E,G); 20 μm in H (applies to B,D,F,H).

reorganization of dentate granules cells and CA1–CA3 pyramidal cells develops during the chronic stage.

VGAT changes may reflect changes in the activity of the hippocampal GABAergic network during development of pilocarpine-induced epilepsy

Our results demonstrate, as early as 1 week after pilocarpine injection, a long-term increase in the immunolabeling of VGAT-containing terminals in all layers of the hippocampal formation. Our interpretation of this finding is that the increased levels of immunoreactivity reflect increased concentrations of VGAT in the terminals resulting from increased VGAT synthesis. This interpretation is based on the fact that we observed a strong parallel between the increased intensity of labeling for VGAT and increased levels of VGAT mRNA in all remaining interneurons. However, we cannot exclude the possibility that the increased levels of VGAT immunoreactivity in the hippocampal formation of pilocarpine-treated animals

could in part reflect an increase in the number of VGAT-containing terminals. In pilocarpine-treated animals, the levels of labeling for VGAT are increased in all regions of the hippocampal formation, including in the inner one-third of the molecular layer and in the lacunosum-moleculare. These differences could reflect an increase in the numbers of terminals in these regions because of a possible axonal sprouting of some surviving GABA neurons. Axonal sprouting has been suggested by previous immunohistochemical studies on the kainate model and human temporal lobe epilepsy tissue (Davenport et al., 1990; Mathern et al., 1995; Wittner et al., 2002). It is difficult at present to distinguish axonal reorganization of remaining GABA neurons from increased levels of VGAT in existing terminals, and both types of changes may occur in the pilocarpine-treated animals. However, a main argument in favor of the increased levels of VGAT in existing terminals rather than axonal sprouting from remaining GABAergic neurons is that we observed this increased in all hippocampal formation, including in two layers in which a loss of GABAergic terminals has been described: the stratum lacunosum-moleculare of CA1 and the outer molecular layer of the dentate gyrus. These losses are due, respectively, to the cell death of a subpopulation of GABAergic neuron in the stratum oriens of CA1, the axons of which project specifically in the stratum lacunosum-moleculare (O-LM cells; Cossart et al., 2001; Dinocourt at al., 2003), and to the loss of a subpopulation of hilar GABAergic neurons, the axons of which project specifically in the outer molecular layer of the dentate gyrus (HICAP cells; Obenaus et al., 1993; Kobayashi and Buckmaster, 2003). A similar increased labeling for GAD67- and GAD65-containing terminals correlated with increased levels of GAD mRNA in interneurons has been described also in these regions in chronic pilocarpine-treated animals (Esclapez and Houser, 1999). Together, these data support a generally increased synthesis of proteins related to the GABAergic neurotransmission rather than axonal sprouting.

Functional implication of VGLUT1 and VGAT reorganizations

Our results strongly support an increased synthesis of VGAT that occurs after status epilepticus and persists until the chronic stage. This increased synthesis is likely to lead to an increased presynaptic performance of the GABAergic transmission. Indeed, it has been demonstrated that the expression levels of vesicular transporters regulate the amounts of neurotransmitter in synaptic vesicles and the efficiency of the neurotransmission. For example, it is known that overexpression or deletion of VGLUTs leads to an increase or decrease, respectively, in intravesicular transmitter content (Fremeau et al., 2004; Wojcik et al., 2004) and that deletion of VGAT leads to a decrease in intravesicular transmitter, leading to a drastic reduction of neurotransmitter release and synaptic transmission (Wojcik et al., 2006). Therefore, an increased synthesis of VGAT is likely to lead to an increased GABA release from all remaining GABAergic interneurons. Such increased GABA release has been previously suggested in several studies that demonstrate increased expression levels of the two GABA-synthesizing enzymes, GAD65 and GAD67, in chronic pilocarpine-treated animals (Esclapez and Houser, 1999). In vitro biochemical studies have demonstrated a strong functional and structural coupling between the synthesis of GABA by membrane-associated GAD (mainly GAD65) and its packaging into synaptic vesicles by VGAT. VGAT forms a protein complex with GAD on the synaptic vesicle. The formation of this complex ensures an efficient coupling between GABA synthesis and packaging into the synaptic vesicles. Furthermore, the studies demonstrate that the activities of synaptic vesicle-associated GAD and VGAT are coupled; indeed, inhibition of GAD decreases VGAT activity (Jin et al., 2003). The demonstration of increased expression for both VGAT (present study) and GAD (Esclapez and Houser, 1999) in remaining interneurons of pilocarpine-treated rats further supports a coregulation of these proteins in vivo.

Such increased expression of proteins involved in presynaptic GABAergic transmission could be associated with increased physiological activity of remaining interneurons. This hypothesis is supported by electrophysiological studies showing that, in chronic pilocarpine-treated animals, interneurons are hyperactive. Spontaneous interictal activity has been recorded in interneurons (Esclapez et al., 1997; Hirsch et al., 1999; Cossart et al., 2001), and the spontaneous firing frequencies of interneurons are higher in chronic pilocarpine-treated animals than in control rats (Cossart et al., 2001). This increased activity of remaining interneurons is likely already to occur during the latent period, as reported in the pilocarpine (El-Hassar et al., 2007) and kainate (Shao and Dudek, 2005) models. Such a response from remaining interneurons has been suggested to reflect an adaptive mechanism to compensate for the loss of hilar and stratum oriens CA1 interneurons in order to prevent an excessive firing of the principal cells. However, remaining interneurons are unlikely to provide precisely the same types of controls as the original population. Indeed, electrophysiological studies have demonstrated that, despite the increased activity of remaining interneurons, a decreased inhibition is present in the distal dendrites of principal cells (Cossart et al., 2001; Kobayashi and Buckmaster, 2003; El-Hassar et al., 2007). Therefore, this change is not sufficient to compensate for the loss of interneurons projecting on the distal dendrites of principal cells.

Our present data further demonstrate that the reorganization of remaining GABAergic neurons characterized by increased GABAergic presynaptic activity occurs at the beginning of the latent period, when the animals are free of electroclinical seizures, and not only at the chronic stage, when the animals display spontaneous recurrent seizure. This is an intriguing observation, which suggests that the surviving GABAergic interneurons in the hippocampal formation are already hyperactive during the latent period, when the reorganization of glutamatergic pathways, including axonal sprouting of granule cells and CA1–CA3 pyramidal cells, is not yet established. Such observations suggest that, during the latent period, increased activity of interneurons does not result from an increase of action-potential-dependent excitatory inputs resulting from axonal sprouting of hippocampal principal cells as suggested at the chronic stage (Cossart et al., 2001). This could reflect an enhanced activity within the glutamatergic pathways that target remaining GABAergic interneurons, including the perforant path, Schaffer collateral from CA3 pyramidal cells, and mossy fibers from dentate granule cells. Such enhanced activity of these glutamatergic pathways has been suggested to occur al-

ready during the latent period and lead to increased frequency of spontaneous excitatory postsynaptic currents (EPSCs) recorded on CA1 pyramidal cell dendrites at this stage (El-Hassar et al., 2007). Analysis of EPSCs and action-potential-independent excitatory currents (mEPSC) on interneurons during the latent period would help to resolve this issue.

Another intriguing observation is that, in contrast to remaining GABAergic interneurons, glutamatergic principal cells do not display an increase of VGLUT1 synthesis in pilocarpine-treated animals, including at the chronic stage (see above). These data suggest that, in vivo, increased physiological activity might not regulate expression levels of VGLUT1 mRNA. Such a difference between the regulations of the VGAT and VGLUT1 expression levels has been reported in other pathological condition in which neuronal excitability is modified, e.g., focal ischemia induced in rat brain (Vemuganti, 2005). All these observations further support clear differences between glutamatergic and GABAergic synaptic transmission regarding the release of a vesicular transmitter pool and its regulation by physiological activity (Moulder and Mennerick, 2005; Moulder et al., 2006). These observations suggest that glutamate release may be subject to greater restraint than GABA release, a mechanism by which neurons can limit the damaging (excitotoxic) effect of glutamate.

Finally, a dual glutamate and GABA phenotype of dentate granule cells has been proposed based on activity-dependent up-regulation of VGAT mRNA in the dentate gyrus and mossy fibers synaptosomes in the kindling model (Lamas et al., 2001). Our data do not provide a basis for speculation that granule cells might have a dual glutamate-GABA phenotype in epileptic animals. Indeed, we do not observe VGAT expression (mRNA and protein) in dentate granule cells of pilocarpine-treated animals, in keeping with the data reported for the kainate model (Sperk et al., 2003). In these two models, spontaneous seizures do not induce any VGAT expression in granule cells.

CONCLUSIONS

This study on the localization and regulation of VGLUT1 and VGAT demonstrates that the glutamatergic and GABAergic networks display different types and time courses of reorganizations during development of pilocarpine-induced temporal lobe epilepsy. During the latent period, when the animals are still free of spontaneous electroclinical seizures, the hippocampal formation already displays a marked reorganization of the intrinsic glutamatergic and GABAergic networks, including a loss of vulnerable glutamatergic and GABAergic neurons and a striking increase in GABAergic presynaptic transmission of all remaining interneurons. These changes precede the structural reorganization of glutamatergic networks and the emergence of spontaneous seizures.

LITERATURE CITED

Amaral DG. 1978. A Golgi study of cell types in the hilar region of the hippocampus in the rat. J Comp Neurol 182:851–914.

Babb TL, Kupfer WR, Pretorius JK, Crandall PH, Levesque MF. 1991. Synaptic reorganization by mossy fibers in human epileptic fascia dentata. Neuroscience 42:351–363.

Baez LA, Eskridge NK, Schein R. 1976. Postnatal development of dopaminergic and cholinergic catalepsy in the rat. Eur J Pharmacol 36:155–162.

Bellocchio EE, Hu H, Pohorille A, Chan J, Pickel VM, Edwards RH. 1998. The localization of the brain-specific inorganic phosphate transporter suggests a specific presynaptic role in glutamatergic transmission. J Neurosci 18:8648–8659.

Bellocchio EE, Reimer RJ, Fremeau RT Jr, Edwards RH. 2000. Uptake of glutamate into synaptic vesicles by an inorganic phosphate transporter. Science 289:957–960.

Bogen IL, Boulland JL, Mariussen E, Wright MS, Fonnum F, Kao HT, Walaas SI. 2006. Absence of synapsin I and II is accompanied by decreases in vesicular transport of specific neurotransmitters. J Neurochem 96:1458–1466.

Boulland J-L, Osen KK, Levy LM, Danbolt NC, Edwards RH, Storm-Mathisen J, Chaudhry FA. 2002. Cell-specific expression of the glutamine transporter SN1 suggests differences in dependence on the glutamine cycle. Eur J Neurosci 15:1615–1631.

Boulland J-L, Qureshi T, Seal R, Rafiki A, Gundersen V, Bergersen L, Fremeau RT Jr, Edwards RH, Storm-Mathisen J, Chaudhry FA. 2004. Expression of the vesicular glutamate transporters during development indicates the widespread co-release of multiple neurotransmitters. J Comp Neurol 480:264–280.

Buckmaster PS, Dudek FE. 1997. Network properties of the dentate gyrus in epileptic rats with hilar neuron loss and granule cell axon reorganization. J Neurophysiol 77:2685–2696.

Buckmaster PS, Wenzel HJ, Kunkel DD, Schwartzkroin PA. 1996. Axon arbors and synaptic connections of hippocampal mossy cells in the rat in vivo. J Comp Neurol 366:271–292.

Buckmaster PS, Zhang GF, Yamawaki R. 2002. Axon sprouting in a model of temporal lobe epilepsy creates a predominantly excitatory feedback circuit. J Neurosci 22:6650–6658.

Cavalheiro EA, Bortolotto ZA, Turski L. 1987. Microinjections of the gamma-aminobutyrate antagonist, bicuculline methiodide, into the caudate-putamen prevent amygdala-kindled seizures in rats. Brain Res 411:370–372.

Cavazos JE, Sutula TP. 1990. Progressive neuronal loss induced by kindling: a possible mechanism for mossy fiber synaptic reorganization and hippocampal sclerosis. Brain Res 527:1–6.

Chang Y-C, Gottlieb DI. 1988. Characterization of the proteins purified with monoclonal antibodies to glutamic acid decarboxylase. J Neurosci 8:2123–2130.

Chaudhry FA, Reimer RJ, Bellocchio EE, Danbolt NC, Osen KK, Edwards RH, Storm-Mathisen J. 1998. The vesicular GABA transporter, VGAT, localizes to synaptic vesicles in sets of glycinergic as well as GABAergic neurons. J Neurosci 18:9733–9750.

Cossart R, Dinocourt C, Hirsch JC, Merchan-Perez A, De FJ, Ben-Ari Y, Esclapez M, Bernard C. 2001. Dendritic but not somatic GABAergic inhibition is decreased in experimental epilepsy. Nat Neurosci 4:52–62.

Cronin J, Dudek FE. 1988. Chronic seizures and collateral sprouting of dentate mossy fibers after kainic acid treatment in rats. Brain Res 474:181–184.

Davenport CJ, Brown WJ, Babb TL. 1990. Sprouting of GABAergic and mossy fiber axons in dentate gyrus following intrahippocampal kainate in the rat. Exp Neurol 109:180–190.

Dinocourt C, Petanjek Z, Freund TF, Ben-Ari Y, Esclapez M. 2003. Loss of interneurons innervating pyramidal cell dendrites and axon initial segments in the CA1 region of the hippocampus following pilocarpine-induced seizures. J Comp Neurol 459:407–425.

El-Hassar L, Milh M, Wendling F, Ferrand N, Esclapez M, Bernard C. 2007. Cell domain-dependent changes in the glutamatergic and GABAergic drives during epileptogenesis in the rat CA1 region. J Physiol 578:193–211.

Esclapez M, Houser CR. 1999. Up-regulation of GAD65 and GAD67 in remaining hippocampal GABA neurons in a model of temporal lobe epilepsy. J Comp Neurol 412:488–505.

Esclapez M, Tillakaratne NJK, Tobin AJ, Houser CR. 1993. Comparative localization of mRNAs encoding two forms of glutamic acid decarboxylase with nonradioactive in situ hybridization methods. J Comp Neurol 331:339–362.

Esclapez M, Tillakaratne NJ, Kaufman DL, Tobin AJ, Houser CR. 1994. Comparative localization of two forms of glutamic acid decarboxylase and their mRNAs in rat brain supports the concept of functional differences between the forms. J Neurosci 14:1834–1855.

Esclapez M, Hirsch JC, Khazipov R, Ben Ari Y, Bernard C. 1997. Operative GABAergic inhibition in hippocampal CA1 pyramidal neurons in experimental epilepsy. Proc Natl Acad Sci U S A 94:12151–12156.

Esclapez M, Hirsch JC, Ben Ari Y, Bernard C. 1999. Newly formed excitatory pathways provide a substrate for hyperexcitability in experimental temporal lobe epilepsy. J Comp Neurol 408:449–460.

Ferhat L, Esclapez M, Represa A, Fattoum A, Shirao T, Ben-Ari Y. 2003. Increased levels of acidic calponin during dendritic spine plasticity after pilocarpine-induced seizures. Hippocampus 13:845–858.

Fremeau RT, Troyer MD, Pahner I, Nygaard GO, Tran CH, Reimer RJ, Bellocchio EE, Fortin D, Storm-Mathisen J, Edwards RH. 2001. The expression of vesicular glutamate transporters defines two classes of excitatory synapse. Neuron 31:247–260.

Fremeau RT Jr, Kam K, Qureshi T, Johnson J, Copenhagen DR, Storm-Mathisen J, Chaudhry FA, Nicoll RA, Edwards RH. 2004. Vesicular glutamate transporters 1 and 2 target to functionally distinct synaptic release sites. Science 304:1815–1819.

Gulyas AI, Toth K, McBain CJ, Freund TF. 1998. Stratum radiatum giant cells: a type of principal cell in the rat hippocampus. Eur J Neurosci 10:3813–3822.

Hirsch JC, Agassandian C, Merchan-Perez A, Ben Ari Y, DeFelipe J, Esclapez M, Bernard C. 1999. Deficit of quantal release of GABA in experimental models of temporal lobe epilepsy. Nat Neurosci 2:499–500.

Hoëltke HJ, Kessler C. 1990. Nonradioactive labeling of RNA transcripts in vitro with the hapten digoxigenin (DIG); hybridization and ELISA-based detection. Nucleic Acids Res 18:5843–5851.

Houser CR, Esclapez M. 1994. Localization of mRNAs encoding two forms of glutamic acid decarboxylase in the rat hippocampal formation. Hippocampus 4:530–545.

Houser CR, Esclapez M. 1996. Vulnerability and plasticity of the GABA system in the pilocarpine model of spontaneous recurrent seizures. Epilepsy Res 26:207–218.

Houser CR, Miyashiro JE, Swartz BE, Walsh GO, Rich JR, Gado-Escueta AV. 1990. Altered patterns of dynorphin immunoreactivity suggest mossy fiber reorganization in human hippocampal epilepsy. J Neurosci 10:267–282.

Jin H, Wu H, Osterhaus G, Wei J, Davis K, Sha D, Floor E, Hsu CC, Kopke RD, Wu JY. 2003. Demonstration of functional coupling between gamma-aminobutyric acid (GABA) synthesis and vesicular GABA transport into synaptic vesicles. PNAS 100:4293–4298.

Kaneko T, Fujiyama F, Hioki H. 2002. Immunohistochemical localization of candidates for vesicular glutamate transporters in the rat brain. J Comp Neurol 444:39–62.

Kaufman DL, Houser CR, Tobin AJ. 1991. Two forms of the gamma-aminobutyric acid synthetic enzyme glutamate decarboxylase have distinct intraneuronal distributions and cofactor interactions. J Neurochem 56:720–723.

Kobayashi M, Buckmaster PS. 2003. Reduced inhibition of dentate granule cells in a model of temporal lobe epilepsy. J Neurosci 15:2440–2452.

Lamas M, Gomez-Lira G, Gutierrez R. 2001.Vesicular GABA transporter mRNA expression in the dentate gyrus and in mossy fiber synaptosomes. Brain Res Mol Brain Res 30:209–214.

Lehmann TN, Gabriel S, Eilers A, Njunting M, Kovacs R, Schulze K, Lanksch WR, Heinemann U. 2001. Fluorescent tracer in pilocarpine-treated rats shows widespread aberrant hippocampal neuronal connectivity. Eur J Neurosci 14:83–95.

Liu Y, Fujise N, Kosaka T. 1996. Distribution of calretinin immunoreactivity in the mouse dentate gyrus. I. General description. Exp Brain Res 108:389–403.

Lu W, Haber SN. 1992. In situ hybridization histochemistry: a new method for processing material stored for several years. Brain Res 578:155–160.

Lynch M, Sutula T. 2000. Recurrent excitatory connectivity in the dentate gyrus of kindled and kainic acid-treated rats. J Neurophysiol 82:693–704.

Maccaferri G, McBain CJ. 1996. Long-term potentiation in distinct subtypes of hippocampal nonpyramidal neurons. J Neurosci 16:5334–5343.

Masukawa LM, O'Connor WM, Burdette LJ, McGonigle P, Sperling MR, O'Connor MJ, Uruno K. 1997. Mossy fiber reorganization and its possible physiological consequences in the dentate gyrus of epileptic humans. Adv Neurol 72:53–68.

Mathern GW, Babb TL, Pretorius JK, Leite JP. 1995. Reactive synaptogenesis and neuron densities for neuropeptide Y, somatostatin, and glutamate decarboxylase immunoreactivity in the epileptogenic human fascia dentata. J Neurosci 15:3990–4004.

McCloskey DP, Hintz TM, Pierce JP, Scharfman HE. 2006. Stereological methods reveal the robust size and stability of ectopic hilar granule cells after pilocarpine-induced status epilepticus in the adult rat. Eur J Neurosci 24:2203–2210.

McIntire SL, Reimer RJ, Schuske K, Edwards RH, Jorgensen EM. 1997. Identification and characterization of the vesicular GABA transporter. Nature 389:870–876.

Mello LE, Cavalheiro EA, Tan AM, Kupfer WR, Pretorius JK, Babb TL, Finch DM. 1993. Circuit mechanisms of seizures in the pilocarpine model of chronic epilepsy: cell loss and mossy fiber sprouting. Epilepsia 34:985–995.

Miyazaki T, Fukaya M, Shimizu H, Watanabe M. 2003. Subtype switching of vesicular glutamate transporters at parallel fibre-Purkinje cell synapses in developing mouse cerebellum. Eur J Neurosci 17:2563–2572.

Molnar P, Nadler JV. 1999. Mossy fiber-granule cell synapses in the normal and epileptic rat dentate gyrus studied with minimal laser photostimulation. J Neurophysiol 82:1883–1894.

Moulder KL, Mennerick S. 2005. Reluctant vesicles contribute to the total readily releasable pool in glutamatergic hippocampal neurons. J Neurosci 25:3842–3850.

Moulder KL, Jiang X, Taylor AA, Olney JW, Mennerick S. 2006. Physiological activity depresses synaptic function through an effect on vesicle priming. J Neurosci 26:6618–6626.

Nadler JV, Perry BW, Cotman CW. 1980. Selective reinnervation of hippocampal area CA1 and the fascia dentata after destruction of CA3–CA4 afferents with kainic acid. Brain Res 182:1–9.

Obenaus A, Esclapez M, Houser CR. 1993. Loss of glutamate decarboxylase mRNA-containing neurons in the rat dentate gyrus following pilocarpine-induced seizures. J Neurosci 13:4470–4485.

Okazaki MM, Nadler JV. 2001. Glutamate receptor involvement in dentate granule cell epileptiform activity evoked by mossy fiber stimulation. Brain Res 915:58–69.

Okazaki MM, Evenson DA, Nadler JV. 1995. Hippocampal mossy fiber sprouting and synapse formation after status epilepticus in rats: visualization after retrograde transport of biocytin. J Comp Neurol 352: 515–534.

Parent JM, Yu TW, Leibowitz RT, Geschwind DH, Sloviter RS, Lowenstein DH. 1997. Dentate granule cell neurogenesis is increased by seizures and contributes to aberrant network reorganization in the adult rat hippocampus. J Neurosci 17:3727–3738.

Parent JM, Elliott RC, Pleasure SJ, Barbaro NM, Lowenstein DH. 2006. Aberrant seizure-induced neurogenesis in experimental temporal lobe epilepsy. Ann Neurol 59:81–91.

Persson S, Boulland JL, Aspling M, Larsson M, Fremeau RT, Edwards RH, Storm-Mathisen J, Chaudhry FA, Broman J. 2006. Distribution of vesicular glutamate transporters 1 and 2 in the rat spinal cord, with a note on the spinocervical tract. J Comp Neurol 497:683–701.

Pothos EN, Larsen KE, Krantz DE, Liu Y, Haycock JW, Setlik W, Gershon MD, Edwards RH, Sulzer D. 2000. Synaptic vesicle transporter expression regulates vesicle phenotype and quantal size. J Neurosci 20:7297–7306.

Represa A, Jorquera I, Le Gal LS, Ben Ari Y. 1993. Epilepsy induced collateral sprouting of hippocampal mossy fibers: does it induce the development of ectopic synapses with granule cell dendrites? Hippocampus 3:257–268.

Sagné C, El Mestikawy S, Isambert MF, Hamon M, Henry JP, Giros B, Gasnier B. 1997. Cloning of a functional vesicular GABA and glycine transporter by screening of genome databases. FEBS Lett 417:177–183.

Scharfman HE, Goodman JH, Sollas AL. 2000. Granule-like neurons at the hilar/CA3 border after status epilepticus and their synchrony with area CA3 pyramidal cells: functional implications of seizure-induced neurogenesis. J Neurosci 20:6144–6158.

Scharfman HE, Smith KL, Goodman JH, Sollas AL. 2001. Survival of dentate hilar mossy cells after pilocarpine-induced seizures and their synchronized burst discharges with area CA3 pyramidal cells. Neuroscience 104:741–759.

Scharfman HE, Sollas AL, Berger RE, Goodman JH. 2003. Electrophysiological evidence of monosynaptic excitatory transmission between granule cells after seizure-induced mossy fiber sprouting. J Neurophysiol 90:2536–2547.

Schwarzer C, Sperk G. 1995. Hippocampal granule cells express glutamic

acid decarboxylase-67 after limbic seizures in the rat. Neuroscience 69:705–709.

Shao LR, Dudek FE. 2005. Changes in mIPSCs and sIPSCs after kainate treatment: evidence for loss of inhibitory input to dentate granule cells and possible compensatory responses. J Neurophysiol 94:952–960.

Sloviter R, Nilaver G. 1987. Immunocytochemical localization of GABA-, cholecystokinin-, vasoactive intestinal polypeptide-, and somatostatin-like immunoreactivity in the area dentata and hippocampus of the rat. J Comp Neurol 256:42–60.

Sloviter RS, Dichter MA, Rachinsky TL, Dean E, Goodman JH, Sollas AL, Martin DL. 1996. Basal expression and induction of glutamate decarboxylase and GABA in excitatory granule cells of the rat and monkey hippocampal dentate gyrus. J Comp Neurol 373:593–618.

Sloviter RS, Zappone CA, Harvey BD, Bumanglag AV, Bender RA, Frotscher M. 2003. "Dormant basket cell" hypothesis revisited: relative vulnerabilities of dentate gyrus mossy cells and inhibitory interneurons after hippocampal status epilepticus in the rat. J Comp Neurol 459:44–76.

Song H, Ming G, Fon E, Bellocchio E, Edwards RH, Poo M. 1997. Expression of a putative vesicular acetylcholine transporter facilitates quantal transmitter packaging. Neuron 18:815–826.

Soriano E, Frotscher M. 1993. Spiny nonpyramidal neurons in the CA3 region of the rat hippocampus are glutamate-like immunoreactive and receive convergent mossy fiber input. J Comp Neurol 333:435–448.

Soriano E, Frotscher M. 1994. Mossy cells of the rat fascia dentata are glutamate-immunoreactive. Hippocampus 4:65–69.

Sperk G, Schwarzer C, Heilman J, Furtinger S, Reimer RJ, Edwards RH, Nelson N. 2003. Expression of plasma membrane GABA transporters but not of the vesicular GABA transporter in dentate granule cells after kainic acid seizures. Hippocampus 13:806–815.

Sutula T, Zhang P, Lynch M, Sayin U, Golarai G, Rod R. 1998. Synaptic and axonal remodeling of mossy fibers in the hilus and supragranular region of the dentate gyrus in kainate-treated rats. J Comp Neurol 390:578–594.

Travis ER, Wang YM, Michael DJ, Caron MG, Wightman RM. 2000. Differential quantal release of histamine and 5-hydroxytryptamine from mast cells of vesicular monoamine transporter 2 knockout mice. Proc Natl Acad Sci U S A 97:162–167.

Turski WA, Cavalheiro EA, Schwarz M, Czuczwar SJ, Kleinrok Z, Turski L. 1983. Limbic seizures produced by pilocarpine in rats—behavioral, electroencephalographic and neuropathological study. Behav Brain Res 9:315–335.

Vemuganti R. 2005. Decreased expression of vesicular GABA transporter, but not vesicular glutamate, acetylcholine and monoamine transporters in rat brain following focal ischemia. Neurochem Int 47:136–142.

Watson RE Jr., Wiegand SJ, Clough RW, Hoffman GE. 1986. Use of cryoprotectant to maintain long-term peptide immunoreactivity and tissue morphology. Peptides 7:155–159.

Wenzel HJ, Buckmaster PS, Anderson NL, Wenzel ME, Schwartzkroin PA. 1997. Ultrastructural localization of neurotransmitter immunoreactivity in mossy cell axons and their synaptic targets in the rat dentate gyrus. Hippocampus. 7:559–70.

Wenzel HJ, Woolley CS, Robbins CA, Schwartzkroin PA. 2000. Kainic acid-induced mossy fiber sprouting and synapse formation in the dentate gyrus of rats. Hippocampus 10:244–260.

Wittner L, Eross L, Szabo Z, Toth S, Czirjak S, Halasz P, Freund TF, Magloczky ZS. 2002. Synaptic reorganization of calbindin-positive neurons in the human hippocampal CA1 region in temporal lobe epilepsy. Neuroscience 115:961–978.

Wojcik SM, Rhee JS, Herzog E, Sigler A, Jahn R, Takamori S, Brose N, Rosenmund C. 2004. An essential role for vesicular glutamate transporter 1 (VGLUT1) in postnatal development and control of quantal size. Proc Natl Acad Sci U S A 101:7158–7163.

Wojcik SM, Katsurabayashi S, Guillemin I, Friauf E, Rosenmund C, Brose N, Rhee JS. 2006. A shared vesicular carrier allows synaptic corelease of GABA and glycine. Neuron 50:575–587.

Wuarin JP, Dudek FE. 1996. Electrographic seizures and new recurrent excitatory circuits in the dentate gyrus of hippocampal slices from kainate-treated epileptic rats. J Neurosci 16:4438–4448.

Wuarin JP, Dudek FE. 2001. Excitatory synaptic input to granule cells increases with time after kainate treatment. J Neurophysiol 85:1067–1077.